Adaptation to a Viscous Snowball Earth Ocean as a Path to Complex Multicellularity

Carl Simpson*

University of Colorado Museum of Natural History and Department of Geological Sciences, University of Colorado, Boulder, Colorado 80309

ABSTRACT: Animals, fungi, and algae with complex multicellular bodies all evolved independently from unicellular ancestors. The early history of these major eukaryotic multicellular clades, if not their origins, co-occur with an extreme phase of global glaciations known as the Snowball Earth. Here, I propose that the long-term loss of low-viscosity environments due to several rounds global glaciation drove the multiple origins of complex multicellularity in eukaryotes and the subsequent radiation of complex multicellular groups into previously unoccupied niches. In this scenario, life adapts to Snowball Earth oceans by evolving large size and faster speeds through multicellularity, which acts to compensate for high-viscosity seawater and achieve fluid flow at sufficient levels to satisfy metabolic needs. Warm, low-viscosity seawater returned with the melting of the Snowball glaciers, and with it, by virtue of large and fast multicellular bodies, new ways of life were unveiled.

Keywords: Metazoa, macroalgae, division of labor, Neoproterozoic, fluid dynamics.

Introduction

Since its origin, unicellular life clustered together to form simple groups (Butterfield 2009). Despite the long history of mats, stromatolites, and biofilms constructed by groups of microbes, complex multicellularity never arose in bacteria or archaea (Bonner 2001). It even took more than 1 billion years for large and complex multicellular life to arise in eukaryotes (Butterfield 2009; Knoll 2011; Cohen and Macdonald 2015; Valentine and Marshall 2015). But by the end of the Neoproterozoic era, large and complex eukaryotic life had evolved independently in several clades (Bonner 2001; Grosberg and Strathmann 2007; Knoll 2011; Herron et al. 2013; Niklas and Newman 2013; Del Cortona et al. 2020). These diverse multicellular organisms soon became ecologically important (Bambach et al. 2007; Yuan et al. 2011, 2013; Liu et al. 2015; Butterfield 2018; Darroch et al. 2018), setting the stage for the Cambrian explosion of skeletonized and bilaterian animals and their subsequent radiation (Valentine et al. 1991; Erwin et al. 2011; Budd and Jensen 2017). The long delay of the origin of complex multicellularity, characterized by large size, division of labor, and spatial organization (Knoll 2011), and its multiple coincident eukaryotic origins suggest that a change in the environment was important.

It has long been thought that the rise of oxygen controlled the origin of complex multicellularity (for an excellent review and critique, see Mills and Canfield 2014), such that the origin and evolution of complex multicellularity was prohibited until sufficient levels of oxygen accumulated in the atmosphere (Nursall 1959; Raff and Raff 1970; Towe 1970; Rhoads and Morse 1971; Cloud 1976; Knoll and Carroll 1999; Knoll 2011). However, it has become clear that low oxygen levels may not constrain the origin of complex multicellular groups as much as expected (Knoll and Sperling 2014; Mentel et al. 2014; Mills and Canfield 2014; Mills et al. 2014, 2018; Butterfield 2018; Leys and Kahn 2018; Cole et al. 2020). Oxygen suppresses macroscopic multicellularity in experimentally evolved multicellular yeast (Bozdag et al. 2021). Animals such as sponges, ctenophores, and cnidarians have low metabolic needs (Mills et al. 2014, 2018), and sponges, ctenophores, and cnidarians have a remarkable ability to move large volumes of water (De Goeij et al. 2013; Leys and Kahn 2018), which may reverse the causal arrow linking body size and oxygen. Large sizes may not arise as a result of higher oxygen levels, but rather large size may provide basal animals with a mechanism to extract more oxygen from the environment than expected in low atmospheric concentrations.

Surface area–to–volume arguments link size to oxygen levels during the origin of complex multicellularity (Knoll 2011; Knoll and Hewitt 2011). Whatever the absolute

oxygen levels were during the Neoproterozoic, they are likely to have an increasing trend over this span of time (Cole et al. 2020). Consequently, if the oxygen hypothesis is the only mechanism at work, then organismal body sizes should increase over geological time in step with the rising level of oxygen.

Predation has also been proposed to be important in the origins of multicellularity (Stanley 1973; Herron et al. 2019). But because low oxygen limits carnivory (Sperling et al. 2013) and the likely persistence of low oxygen until after the Cambrian explosion (Sperling et al. 2015), it seems that an escalation in size produced by predation may not be so important in the origins of animal multicellularity. Moreover, in modern systems unicellular algae limit size escalation by protist predation because the algal prey achieve protective large size by swelling up, which acts to lower their nutritive value and curtails any arms races (Branco et al. 2020). There is also a long history of protistan predation recorded in the fossil record (Porter et al. 2003; Cohen et al. 2011; Porter 2011, 2016; Cohen and Riedman 2018; Mills 2020) that coincided with simple multicellularity (cellular colonies); nevertheless, a half-billion-year lag remains until the origins of complex multicellularity. Given all of these recent discoveries, it seems unlikely for predation to be a major driver of the origin of large and complex multicellularity.

Recently, Brocks et al. (2017) proposed that an increase in nutrients (particularly phosphorus) led to a radiation of algae and consequently to the origin of animals. While increasing nutrients is clearly important for increasing population carrying capacities, it is not clear how complex multicellularity is a consequence of more nutrients. Stanley's (1973) argument about the role of predation hints at a vague but possible probabilistic mechanism for nutrient influx—larger populations may lead to more evolution, which may in turn increase the probability of evolving complex multicellularity.

Without oxygen limitation, nutrient influx, or predation pressure as live hypotheses, we lack a potential mechanism for the origins of complex multicellularity. The keys to understanding the origin of complex multicellularity lie in identifying the evolutionary cause of increased size and determining why the major groups of multicellular life originated during the Neoproterozoic era.

During the Cryogenian period of the Neoproterozoic, at least two (and possibly three or more) global glaciations, together known as the Snowball Earth, saw the planet covered with a thick layer of ice for a sum total of 70 million years (Macdonald et al. 2010; MacLennan et al. 2020). Cold equatorial conditions began by 751 million years ago, prior to the main phases of global glaciations (MacLennan et al. 2020). Snowball Earth glaciations would influence many aspects of the geochemical and physical environments relevant to life (Pierrehumbert et al. 2011). However, it can

be easy to forget that seawater itself would have undergone dramatic physical shifts during Snowball glaciations, including a dramatic increase in its viscosity (fig. 1). As seawater cools, its viscosity increases dramatically (Dorsey 1968; Podolsky 1994; Vogel 1996; Sharqawy et al. 2010; Nayar et al. 2016). Increases in salinity also increase viscosity, but the effect pales in comparison to the effects of temperature (Dorsey 1968).

Because of the small sizes of the unicellular life that was abundant prior to Snowball Earth (Heim et al. 2017), increases in viscosity would have drastic effects on the ecology of unicellular life. In this article, I propose that complex multicellularity emerged as an adaptation to the high viscosity of cold Snowball Earth oceans.

Life Survived Snowball Earth

Both geological evidence and climate models suggest that equatorial oceans during Snowball Earth glaciations were cold (Kirschvink 1992; Hoffman et al. 1998; Pierrehumbert et al. 2011). Ice up to 1 km thick covered both land and oceans from the poles to the equator and potentially cut off the oceans from sunlight (Hoffman et al. 1998, 2017).

The Snowball Earth glaciations should have caused a mass extinction (Hoffman et al. 1998), but there are a surprisingly large number of potential range-through taxa, at least at higher taxonomic levels (Corsetti et al. 2006; Moczydłowska 2008; Javaux 2011; Ye et al. 2015; Riedman and Sadler 2018), and only a slight drop in diversity over this time interval (Riedman et al. 2014; Cohen and Macdonald 2015; Riedman and Sadler 2018). Moreover, because of the homogeneity of the ocean environment during Snowball glaciations (Ashkenazy et al. 2013), survivors would not have been able to track habitats by migration because the majority of habitats would have vanished. Given this and the long 70-million-year duration of cold equatorial seas (Macdonald et al. 2010; MacLennan et al. 2020), life likely adapted to Snowball conditions.

We see an inter- and postglacial diversification of biomarkers indicating an increased abundance of eukaryotic algae (Brocks et al. 2017) and sponges (Love et al. 2009; Love and Summons 2015). Centimeter-scale body fossils of diverse algae (Cohen et al. 2015; Ye et al. 2015) and "Twitya discs," including the form taxon *Aspidella*, make their first appearances in the interval between the Sturtian and Marinoan glaciations (Hofmann et al. 1990; Narbonne 1994; Sperling et al. 2016; Burzynski et al. 2020).

In the Ediacaran, after the Snowball Earth glaciations and when warm seawaters returned, animals, algae, and many other multicellular clades with complex organization, including members of the enigmatic Ediacaran fauna, are abundant in the fossil record (Love et al. 2009; Erwin et al. 2011; Knoll 2011; Cohen and Macdonald 2015; dos
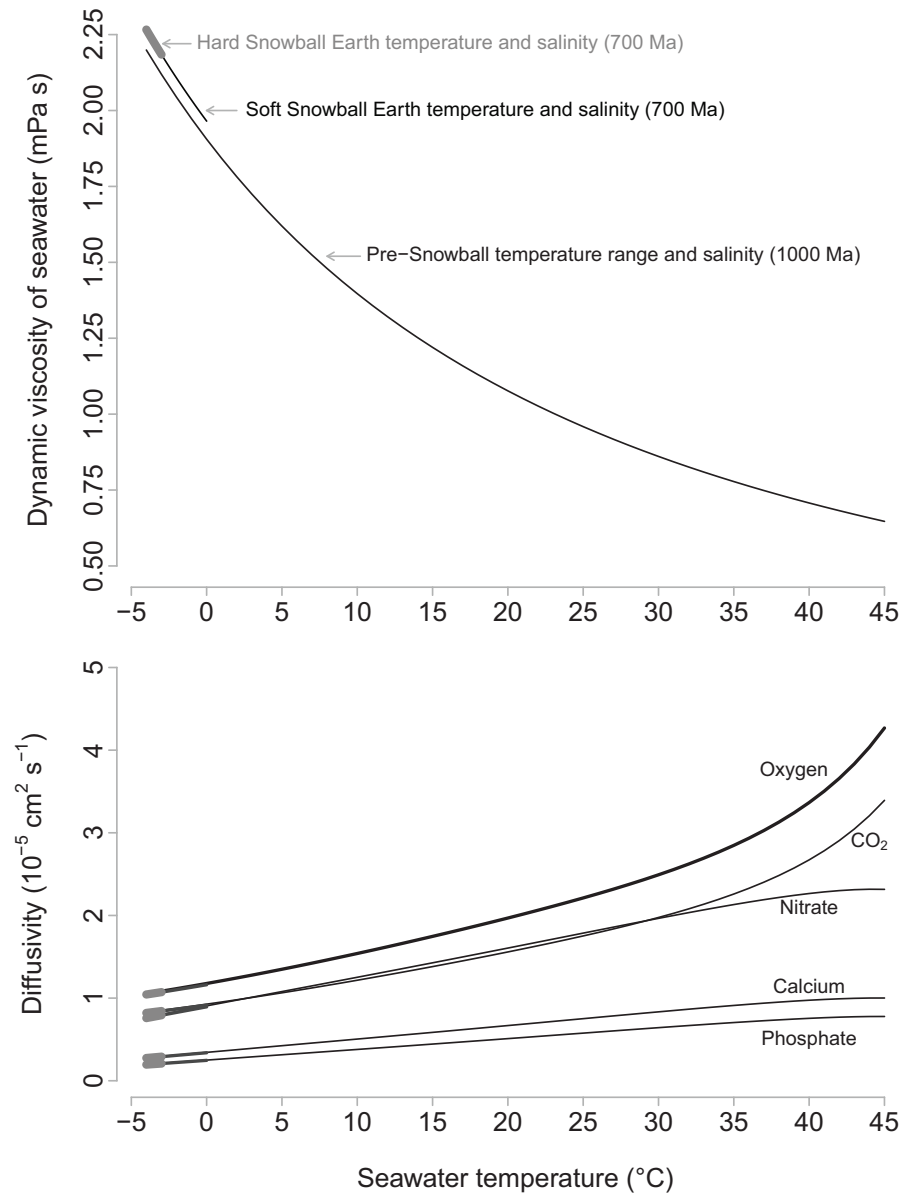
Figure 1: Dynamic viscosity and diffusivity profiles of seawater for preglacial and Snowball Earth oceans. Viscosities and diffusivities are based on reconstructed sea-surface temperatures and salinities for preglacial (−4°C through 45°C, 35‰ salinity) and for soft (−4°C through 0°C, 50‰ salinity) and hard (−4°C through −3°C, 50‰ salinity) Snowball oceans. Dynamic viscosity is shown in units of millipascal seconds (mPa s). The bottom panel shows diffusivity for a variety of biologically important molecules. The ranges for hard and soft Snowball conditions is indicated by thickened lines in both panels.

Reis et al. 2015; Love and Summons 2015; Ye et al. 2015; Brocks et al. 2017; Del Cortona et al. 2020).

How Viscous Were Snowball Earth Oceans?

Pre-Snowball circulation models (Fiorella and Sheldon 2017) predict that mean sea surface temperatures in the tropics ranged from 18°C to 30°C with a maximum temperature up to 45°C. Shallow polar and deep ocean water would likely have been cold, near 0°C. As a consequence of this wide range of ocean temperatures, seawater viscosity would have been similarly wide ranging (from about 0.6 to 2.2 mPa s; fig. 1). This great variety of ocean temperatures and viscosities was lost with global glaciation as shallow equatorial waters cooled.

The severity of the Snowball Earth glaciations remain an open question. In the hard Snowball scenario, there is thought to be 1 km of sea ice at the equator (Hoffman

et al. 2017). In the soft Snowball scenario, there would have been cold seawater at the equator, but open ocean would have remained (Abbot et al. 2011). Geological evidence may indicate equatorial cold but ice-free seawater during the Tonian and Cryoginian (MacLennan et al. 2020). For example, giant ooids are common in Neoproterozoic paleoequatorial rock units directly underlaying the glacially derived diamictites (Trower and Grotzinger 2010; Trower 2020). Ooid size arises from the balance between precipitation and abrasion due to wave action (Trower et al. 2017). Cold water changes the precipitation dynamics of calcium carbonate, and high viscosity acts to lower abrasion rates; consequently, Neoproterozoic giant ooids are likely to be paleoenvironmental indicators of cold but ice-free seawater (∼0°C) prior to the onset of both Sturtian and Marinoan glaciations (Trower 2020).

Liquid seawater can become only so cold before freezing; therefore, the temperatures and viscosities of the possible Snowball Earth scenarios converge. Climate models of hard Snowball Earth oceans predict homogeneously cold (nearly −4°C) seawater across all depths and latitudes even for scenarios with up to 1 km of sea ice at the equator (Ashkenazy et al. 2013). The less extreme soft Snowball Earth scenario would have only slightly warmer seawaters, likely near 0°C (Abbot et al. 2011). Higher temperatures are possible locally adjacent to hydrothermal vents, but they would unlikely be refuges for life because of their rarity and the rapid dissipation of heat in the face of cold high-circulation oceans (Ashkenazy et al. 2013).

The low temperatures and high salinities in both Snowball Earth scenarios would yield uniformly high-viscosity seawater (2–2.25 mPa s) across global latitudes and depths (fig. 1). This loss resulted in homogenous oceans across all latitudes and depths (Ashkenazy et al. 2013). In today's oceans, biomass is predominately found in tropical shallow coastal waters and would likely be the same in Precambrian oceans (LaBarbera 1978). Moreover, during any non-Snowball interval of time, marine microorganisms would be able to track their preferred environments as climate changed (e.g., Ajani et al. 2018).

During most of the 80 million years of the Cryogenian, not only would organisms be faced with low temperatures, major geochemical upheavals, and low primary productivity in their life under sea ice (Canfield and Farquhar 2009; Butterfield 2011; Pierrehumbert et al. 2011; Lenton et al. 2014; Hoffman et al. 2017), but shallow tropical species would also be faced with a fundamental change in the consistency of the fluid in which they lived.

Life in Cold Seawater

Unicellular organisms are small, from 0.5 μm to 1 mm in length, with an average of about 80 μm (Fenchel 1987;

Heim et al. 2017), so the way they physically experience ocean water responds to the viscosity brought about by changes in temperature (Purcell 1977; Vogel 1996; Guasto et al. 2012; Goldstein 2015). Food and nutrient capture is paramount for microorganisms, and they can rely on either diffusion or self-generated flows to capture food items and nutrients needed to sustain life (Fenchel 1987). Both diffusion and flow are impacted by cold temperatures. Increases in viscosity directly affect the function of cilia and flagella, impacting unicellular organisms' ability to feed, move, and limit physiological activities that are dependent on ciliary action (Podolsky and Emlet 1993; Podolsky 1994; Gheber et al. 1998; Larsen and Riisgård 2009; Humphries 2013; Qin et al. 2015).

The Péclet number (Pe) quantifies the dominant processes an organism uses to capture nutrients (Vogel 1996). Pe $= vr/D$, where length (r) measures the size of the organism, v is velocity in the fluid relative to the organism, and D is the diffusivity of the nutrient or food within seawater (Guasto et al. 2012; Purcell 1977; Vogel 1996). Organisms with Pe < 1 have ecologies dominated by diffusion, and swimming faster does little to increase the probability of encountering more resources (Vogel 1996). Flow dominates when Pe > 1, and organisms can capture more resources by swimming faster. For comparison's sake, figure 2*A* shows Péclet numbers for bacteria, flagellated eukaryotes, and ciliated eukaryotes (data for bacteria are from Heim et al. [2017] and Kearns [2010]; data for sizes and speeds for eukaryotes are from Lisicki et al. [2019]) for oxygen in 25°C water. Bacterial Péclet numbers are predominately between 0.001 and 0.01, deep within the diffusion-dominated range. For flagellated and ciliated eukaryotes, Pe is larger (0.1 $<$ Pe $<$ 1,000), which highlights how much self-generated flow dominates their ecologies (Fenchel 1987).

For bacteria with small Péclet numbers (Pe < 0.01), the low diffusivity of solutes in cold water would act to increase their Péclet numbers relative to bacteria with the same size and motility in warm water. For oxygen, Pe shifts from an average of 8.6×10^{-3} in 25°C water to 18.4×10^{-3} in −4°C water. Evolving smaller sizes is one way that bacteria can compensate for lower diffusivities and return their Péclet numbers to their normal value in the face of cooling.

For organisms with large Péclet numbers and therefore in a fluid environment dominated by flow, the Reynolds number (Re) quantifies the relative magnitude of inertial to viscous forces that emerge from the interactions among an object's size, its velocity, and the viscous properties of a fluid (Purcell 1977; Vogel 1996). Re $= vr\rho/\mu$, where r measures the size of the organism, v is velocity in the fluid relative to the organism, and ρ and μ are the density and viscosity of seawater, respectively. Recent work on intermediate Reynolds numbers (0.1 $<$ Re $<$ 10) has shown that small changes in Reynolds numbers lead to major
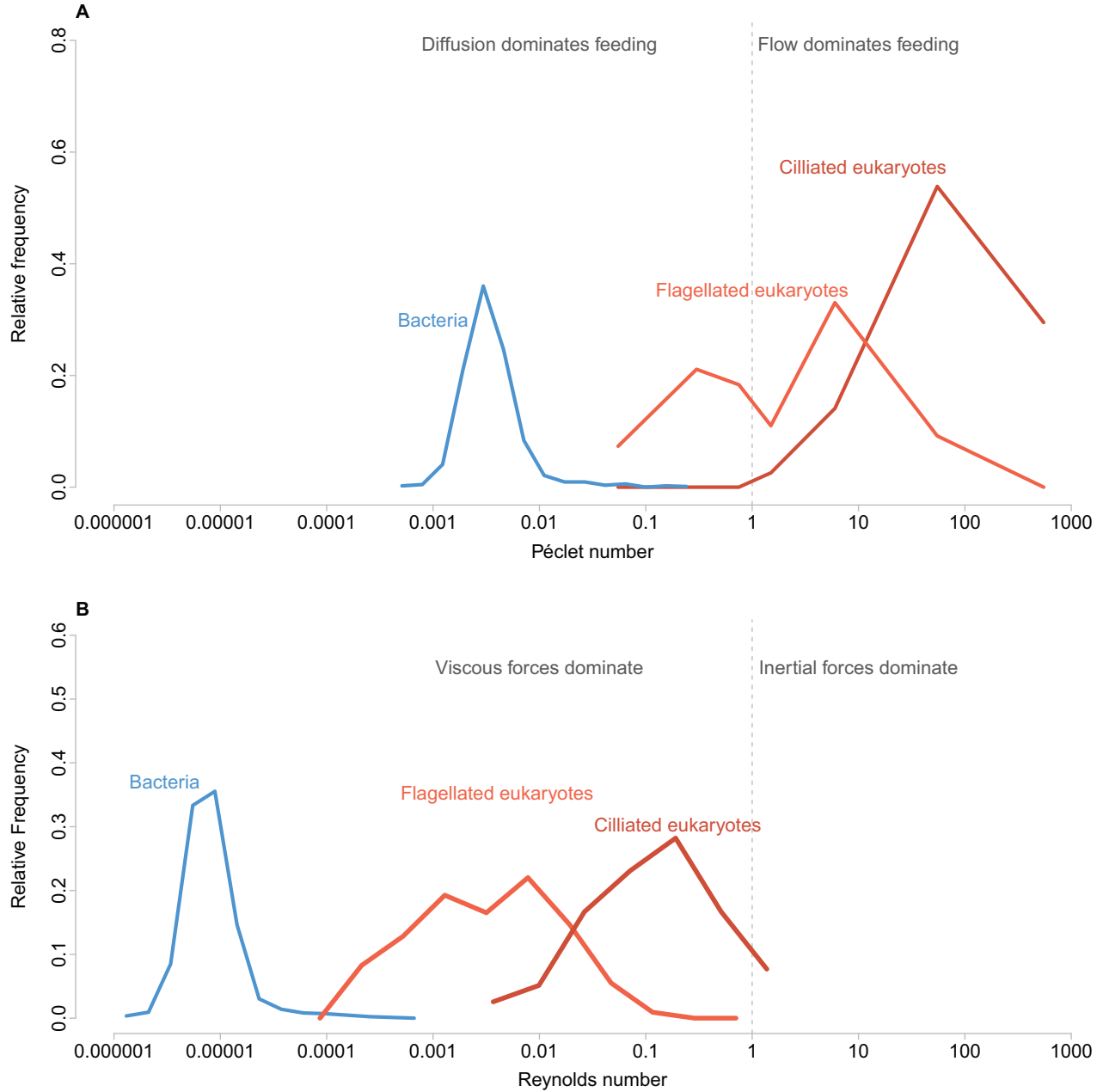
Figure 2: Péclet and Reynolds numbers for bacterial and unicellular eukaryotic species in warm water. *A*, The Péclet number describes the relative balance of flow and diffusion with respect to a resource, in this example, oxygen. *B*, The Reynolds number summarizes the balance of viscous and initial forces. Conditions shown are warm (25°C) with a salinity of 30‰, a diffusivity of O_2 of 2.21×10^{-10} m^2 s^{-1}, and a viscosity of 0.97 mPa s. Flagellated and ciliated eukaryotes are plotted separately because of their different swimming speeds. Data for bacteria from Heim et al. (2017) and Kearns (2010); data for sizes and speeds for eukaryotes are from Lisicki et al. (2019).

changes in the interactions between fluids and objects (Humphries 2009; Klotsa et al. 2015; Dombrowski et al. 2019). In biology, the Reynolds number characterizes how an organism can move, live, and feed within its fluid environment (Purcell 1977; Vogel 1996). Reynolds numbers below 1 indicate a fluid environment dominated by vis-

cous forces, whereas inertial forces dominate for Reynolds numbers larger than 1. Reynolds numbers for bacteria are very low ($\sim$1 $\times$ 10^{-5}; fig. 2*B*). For unicellular eukaryotes, Reynolds numbers are several orders of magnitude higher than those for bacteria due to both the eukaryotes' larger size and their higher swimming speeds. Yet eukaryote

Reynolds numbers are almost all well below 1 (Lisicki et al. 2019), with a median of 0.003 for flagellated eukaryotes and 0.11 for ciliated eukaryotes (fig. 2*B*). For comparisons sake, animals such as adult ctenophores have Reynolds numbers of about 30 (Colin et al. 2020), and the Re of sponge larvae is about 1 (Woollacott 1990; Woollacott 1993).

Over evolutionary time, organisms would be able to evolve different sizes (*r*) or the capability to move faster (*v*) and therefore could control two of the five variables in the Reynolds and Péclet numbers. The other factors—seawater diffusivity (*D*), density (*ρ*), and viscosity (*μ*)—are physically controlled by temperature and salinity and would change as a consequence of Snowball glaciation. Water density (*ρ*) increases only slightly with lower temperatures and higher salinities (Dorsey 1968) and so would not be significantly different from pre-Snowball densities. Viscosity, on the other hand, changes dramatically with temperature (Nayar et al. 2016; Sharqawy et al. 2010; fig. 1) and therefore would have played the dominant role in shifting Reynolds numbers during the Snowball glaciations.

Theoretical and experimental results indicate that motility driven by cilia or flagella is dependent on viscosity (Blake and Sleigh 1974; Sleigh and Blake 1977; Podolsky and Emlet 1993; Humphries 2013) such that $v = \alpha\mu^{-m}$ (Gheber et al. 1998; Larsen and Riisgård 2009; Qin et al. 2015), where α is a constant. The exponent *m* varies among species, with a range between 0.4 and about 4 (Larsen and Riisgård 2009); it is less than 0.5 for bacteria (Humphries 2013) and has been estimated to be nearly 1 for *Chlamydomonas* (Qin et al. 2015). This slowdown occurs because the frequencies at which cilia and flagella move within higher-viscosity water decreases, not because of metabolic sluggishness due to the cold (Podolsky and Emlet 1993; Podolsky 1994; Larsen and Riisgård 2009; Humphries 2013). Consequently, the Péclet numbers for eukaryotes are not expected to differ in warm and cold seawater because cold water lowers diffusivity and attenuates swimming speed via increasing viscosity such that Pe $\sim (\alpha r\rho\mu^{-m})/D$ (fig. 3). Diffusivity declines about as much as viscosity increases, leading to a stable Péclet number for eukaryotes across temperatures.

Substituting the viscosity dependency of speed (assuming $v = \alpha\mu^{-1}$) into the Reynolds numbers for eukaryotes yields Re $= \alpha r\rho/\mu^2$. A doubling of viscosity, as would occur if warm shallow tropical seas become covered in sea ice during the Snowball glaciation, would lead to a steep decline in Reynolds numbers.

Adaptive Strategies in Response to High Viscosity

Because of their large size and motility, eukaryotes have distinctive constraints imposed by viscosity yet depend on fluid flow to access nutrients. Without adaptation, the high viscosity of Snowball seawater would negatively impact motility and therefore feeding and nutrient acquisition. Over evolutionary time, eukaryotes would have potentially been able to evolve different sizes (*r*) or velocities (*v*) to compensate for higher viscosities, as suggested by the Reynolds number. But the Reynolds number does not explicitly track anything of specific biological importance that selection may act on.

Let an organism have an encounter rate (*E*) of a metabolically important nutrient. The encounter rate is a function of the nutrient's concentration (*C*), the organism's velocity relative to seawater (*v*), and the organism's radius (*r*) such that $E = Cv\pi r^2$. Because velocity is a function of viscosity, $v = \alpha\mu^{-m}$, the encounter rate is also a function of viscosity: $E = C\alpha\mu^{-m}\pi r^2$.

In eukaryotes, adding cilia or flagella does not increase motility, nor does increasing cell size lead to a major increase in velocity (Sleigh and Blake 1977; Vogel 2008). Energetics also constrain cilia to be short (Sleigh and Blake 1977; Vogel 2008). Ciliates are much faster than flagellate eukaryotes (Vogel 2008; Lisicki et al. 2019; Wan and Jékely 2021). If ciliates originated prior to the Snowball Earth glaciations (Fernandes et al. 2019)—which the fossil record is equivocal about (e.g., Cohen et al. 2020)—then unicellular eukaryotes with particular forms of cell motility seem to have constrained speeds and would have been unable to evolve velocities where $v > \alpha\mu^{-m}$. This constraint in motility leaves size to the only viable adaptive response for unicellular organisms.

In contrast, multicellularity provides a mechanism to increase both size and speed (Solari et al. 2006; Kiørboe 2011). Metazoan larvae are about twice as large as ciliates and about twice as fast (Lisicki et al. 2019; Montgomery et al. 2019). It is not clear whether the motility mechanism of the last common ancestor of metazoans would have been spongelike, with internal flagella pumping water through chambers, or whether it would have been ctenophore-like (e.g., Whelan et al. 2017), with external cilia-based ctenes. Nevertheless, I consider four estimates for the scaling relationships between speed and size, which can be used as a scaffold for understanding the multicellular transition. Solari et al.(2006) modeled the relationship between size and speed for organisms with *Volvox*-like organization. These colonies are mostly hollow, with somatic cells on the outside and a few germ cells within that give rise to new colonies. Solari and coauthors found that speed scales with the number of cells at about $N^{1/4}$. Sponges have approximately the inverse organization to *Volvox*, where flagella are oriented internally and pores allow water to be pumped through their bodies. For simple sponges, the rate of water flow scales with the volume of the sponge with an exponent of about 0.6 (Morganti et al. 2019), so that the speed of the water through the sponge is proportional to $R^{3\times0.6}$. Pooling
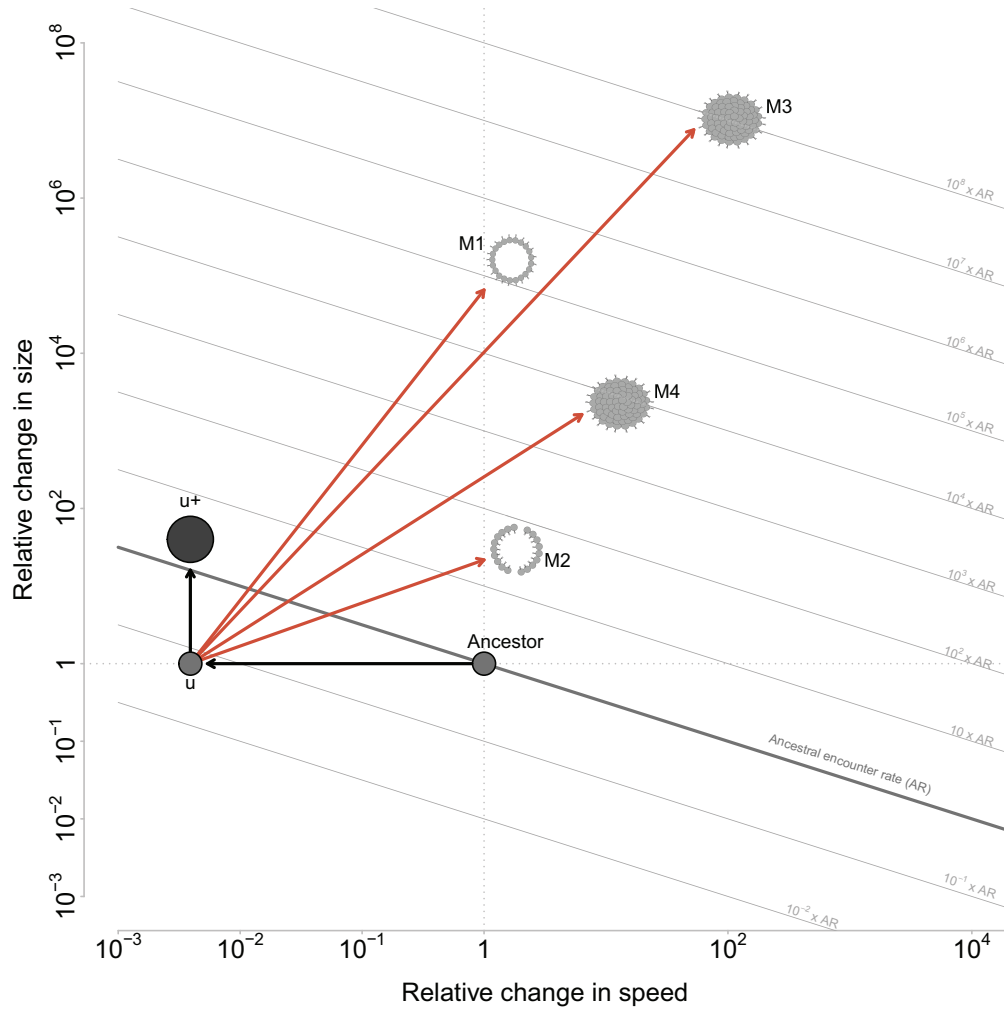
Figure 3: Encounter rates are a function of organism size and swimming speed. The size, speed, and encounter rate of a pre–Snowball Earth unicellular ancestor acts as a reference. The unicellular ancestor will slow down in high viscosity proportional to μ^{-m} (in this figure, $m = 4$) and without adaptation (u) would have a significantly lower encounter rate. One path for unicellular adaptation is to evolve larger size (u+), shown here at the size needed to regain the ancestral encounter rate, but this strategy (along with u) are in a nutrient deficit. Multicellular strategies differ in spatial organization and their size-speed scaling (see text). Here the scaling between speed and viscosity is $m = 4$, which is the case where the encounter rates are equivalent to Reynolds numbers.

speeds and sizes for flagellates, ciliates, metazoan larvae, and volvocales (Solari et al. 2006, 2008; Lisicki et al. 2019; Montgomery et al. 2019) leads to a scaling between the size and speed of $R^{0.6}$. Additionally, Vogel (2008) found a linear scaling relationship between speed and size when invertebrate metazoans are included with unicellular eukaryotes in the regression, so that speed is proportional to R^1. Of course, other size and speed scalings are possible, such as the $R^{0.79}$ scaling depicted by Kiørboe (2011), but they fall between the two scalings I consider here.

A template equation for speed, $v = R^a N^b \alpha \mu^{-m}$, includes the viscosity effect and the scaling between speed and size. The exponents a and b differ for each of the adaptive strategies.

The scaling between metabolic rate and volume of unicellular eukaryotes is approximately equal to 1 (DeLong et al. 2010), so that the metabolic rate (M) of a cell is $M = M_o r^3$. For multicellular organisms things are a little more complex because the metabolic scaling shifts to three-fourths (DeLong et al. 2010). For hollow or sheetlike multicellular organisms or others without internal transport limitation to cells, $M = N r^3$. But for multicellular organisms with internal cells, $M = M_o R^{3 \times 3/4} = M_o R^{9/4}$.

Encounter and metabolic rates scale quantitatively with size and viscosity, and so we can compare the advantages and disadvantages of adaptive strategies to each other. Here, E'/E tracks how increases in viscosity and size effect nutrient acquisition. Likewise, metabolic scaling, M'/M, is

a function of changes in size and tracks the need for nutrients by the constituent cells.

Assuming that the nutrient concentration (C) is constant as Snowball Earth conditions set in and that motility is a function of viscosity such that $v = R^a N^b \alpha \mu^{-m}$, the relative change in encounter rate is

$$\frac{E'}{E} = R^a N^b \left(\frac{\mu'}{\mu}\right)^{-m} \left(\frac{R}{r}\right)^2. \quad (1)$$

Each of the seven adaptive strategies evaluated below will modify this template slightly with specific values of R^a and N^b depending on the particular details of the appropriate size-speed scaling or the number of cells.

Each cell in the cluster individually has a metabolic rate proportional to r^3. The relative change in metabolic rate is a function of the change in the number of cells or their size:

$$\frac{M'}{M} = N\left(\frac{R}{r}\right)^3. \quad (2)$$

If the constituent cells have a radius r, then the number of cells (N) within a multicellular cluster of radius, R, equals $N = (R/r)^2$ for hollow spheres. For unicells, $N = 1$. But for multicellular organisms with internal cells, let us assume that their metabolic rate scales with the total volume with a three-fourths scaling (DeLong et al. 2010):

$$\frac{M'}{M} = \left(\frac{R}{r}\right)^{9/4}. \quad (3)$$

Assuming that unicellular velocities are constrained to be a function of viscosity so that $v = R^0 N^0 \alpha \mu^{-m}$ and that multicellular strategies can have a particular size and speed scaling where $R^a > 1$ or $N^b > 1$, then there are seven broad adaptive strategies to deal with the increased viscosity of the Snowball Earth ocean: (1) no adaptation, so that organisms remain unicellular and cell size remains unchanged (termed u in the following text and figures); (2) the evolution of smaller unicellular size to decrease metabolic demands to match encounter rates (termed u−); (3) the evolution of larger unicellular size to increase encounter rates to compensate for higher viscosity (termed u+); (4) the evolution of larger size through *Volvox*-like multicellularity (termed M1; here, speed scales with size as $N^{1/4}$ and metabolic rate scales with N); (5) the evolution of hollow spongelike multicellularity with internal flow and a speed scaling of $\sim R^{3\times0.6}$, with a metabolic rate that scales with N (termed M2); (6) the evolution of slow-swimming solid multicellularity with speed scaling as $\sim R^{0.6}$ and metabolic scaling as $\sim R^{9/4}$ (termed M3); and (7) the evolution of fast-swimming solid multicellularity with speed scaling as R^1 and metabolic scaling as $\sim R^{9/4}$ (termed M4). Figure 3 shows the encounter rates for each strategy and how they relate to size and speed. Figure 4 shows a phase diagram comparing the metabolic rate and encounter rate for each strategy.

No Adaptation (u)

The most conservative adaptive strategy occurs when organisms remain unicellular ($N = 1$) with no adaptation ($R/r = 1$). Speeds decline as a result of the effect of viscosity and is $v = r^0 1^0 \alpha \mu'^{-m}$. Consequently, the encounter rate is

$$\frac{E'}{E} = \left(\frac{\mu}{\mu'}\right)^m. \quad (4)$$

In this case, because cell size stays the same size ($R = r$), its metabolism remains unchanged:

$$\frac{M'}{M} = \frac{r^3}{r^3} = 1. \quad (5)$$

For this strategy, the unicellular organism has a nutrient deficit of

$$\frac{E'}{M'} = \left(\frac{\mu}{\mu'}\right)^m. \quad (6)$$

The u strategy provides a useful reference to compare other strategies against (figs. 3, 4). For other strategies to have an evolutionary advantage, they must have a lower nutrient deficit than this unicellular strategy.

Smaller Unicells (u−)

If unicellular eukaryotes ($N = 1$) evolve smaller size ($R < r$) in response to increases in viscosity, their encounter rates and metabolic rates will both decrease. The relative change in encounter rate is given by the template equation $E'/E = R^a N^b (\mu'/\mu)^{-m}(R/r)^2$, where $R^a = 1$, $N^b = 1$, and the relative change in metabolic rate is given by $M'/M = (R/r)^3$. For this strategy, the size decrease must lower the metabolic rate enough to match the lowered encounter rate associated with the higher viscosity and the smaller size, where $E'/E = M'/M$. This occurs when $R/r = (\mu/\mu')^m$. Substituting this value of R/r into the equation for E'/E and simplifying gives

$$\frac{E'}{E} = \left(\frac{\mu}{\mu'}\right)^{3m}. \quad (7)$$

By getting smaller, unicellular eukaryotes can reduce their metabolisms sufficiently to maintain nutrient balance ($E'/M' = 1$):

$$\frac{M'}{M} = \left(\frac{R}{r}\right)^3 = \left(\frac{\mu}{\mu'}\right)^{3m}. \quad (8)$$

But to do so they must get significantly smaller, as given by $R/r = (\mu/\mu')^m$, which at the extreme (where $m \approx 4$ and
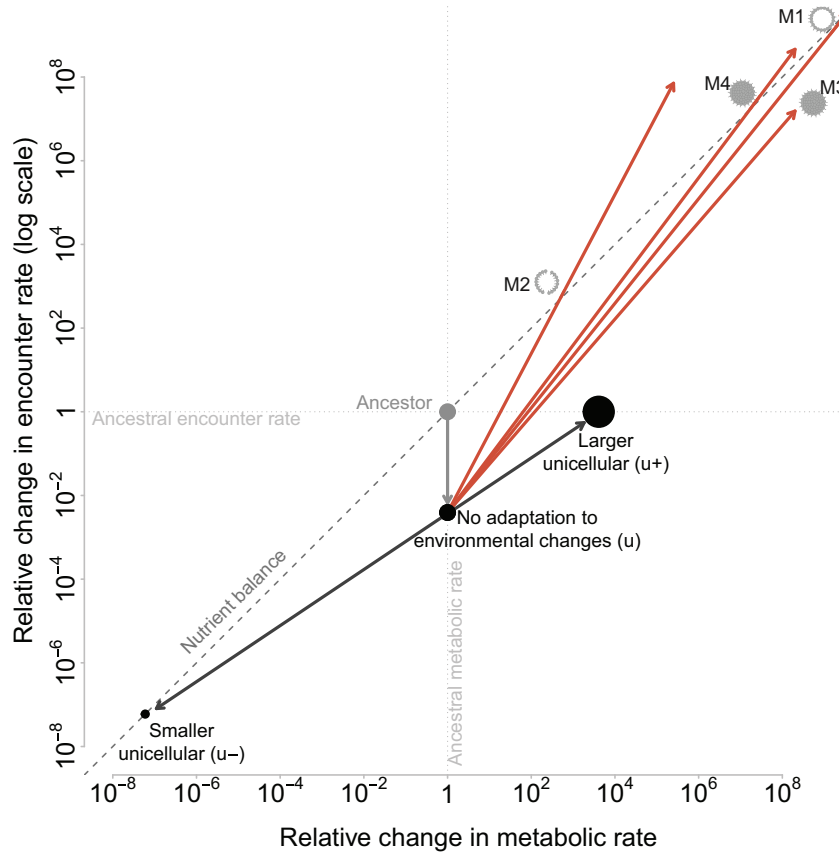
Figure 4: Adaptive strategies that arise as a response to Snowball Earth glaciations. Unicellular strategies are constrained to a single relationship between metabolic rate and encounter rate. Smaller unicells (u−) could evolve that eliminate nutrient deficits, but it requires orders of magnitude decreases in size. Large unicellular strategies (u+) end up increasing nutrient deficits even relative to no adaptation (u). All four multicellular strategies (M1–M4, shown with red arrows) can reach nutrient balance because of increases in size and speed. Strategy M3 reaches nutrient balance beyond the scale shown at a relative change in encounter rate of about 10^{14}.

$\mu/\mu' \approx 1/4$) is a size decrease of a factor of 4^{-4} and a reduction of flow of 4^{-12} (figs. 4, 5). Many picoeukaryotes are less than 3 μm in size and have a broad phylogenetic distribution (e.g., Rocke et al. 2013).

Larger Unicells (u+)

Unicellular eukaryotes ($N = 1$) may evolve larger size ($R > r$), but because there seems to be no correlation with size and speed (Vogel 2008; Lisicki et al. 2019; Montgomery et al. 2019), $R^a = 1$ and $N^b = 1$, and speed declines only with increases in viscosity and does not increase with size. Consequently, their encounter rates and metabolic rates will both increase proportional to size.

The metabolic changes associated with maintaining encounter rates ($E'/E = 1$) provide a useful starting point to understand this strategy. The relative size increase needed for $E' = E$ is $R/r = (\mu'/\mu)^{m/2}$. The relative change in encounter rate is

$$\frac{E'}{E} = \left(\frac{\mu}{\mu'}\right)^{m/2} \left(\frac{\mu'}{\mu}\right)^{m/2} = 1. \tag{9}$$

The relative change in metabolic rate for a unicell of size R is given by its change in volume:

$$\frac{M'}{M} = \left(\frac{R}{r}\right)^3. \tag{10}$$

Because the metabolic rate increases as the cube of the radius but the encounter rate scales with the square of the radius, this strategy suffers from a surface area to volume constraint. Any increase in the encounter rate is matched with a yet greater increase in the metabolic rate (figs. 3, 4). Even if speed scales with size within ciliate and flagellates (and if metazoan larva are included by $\sim R^{0.6}$), nutrient balance is never achieved because of the higher metabolic rates associated with large unicellular organisms. Under these conditions, for nutrient balance to even be possible in the u+ strategy, a size-speed scaling greater than 1 is required.
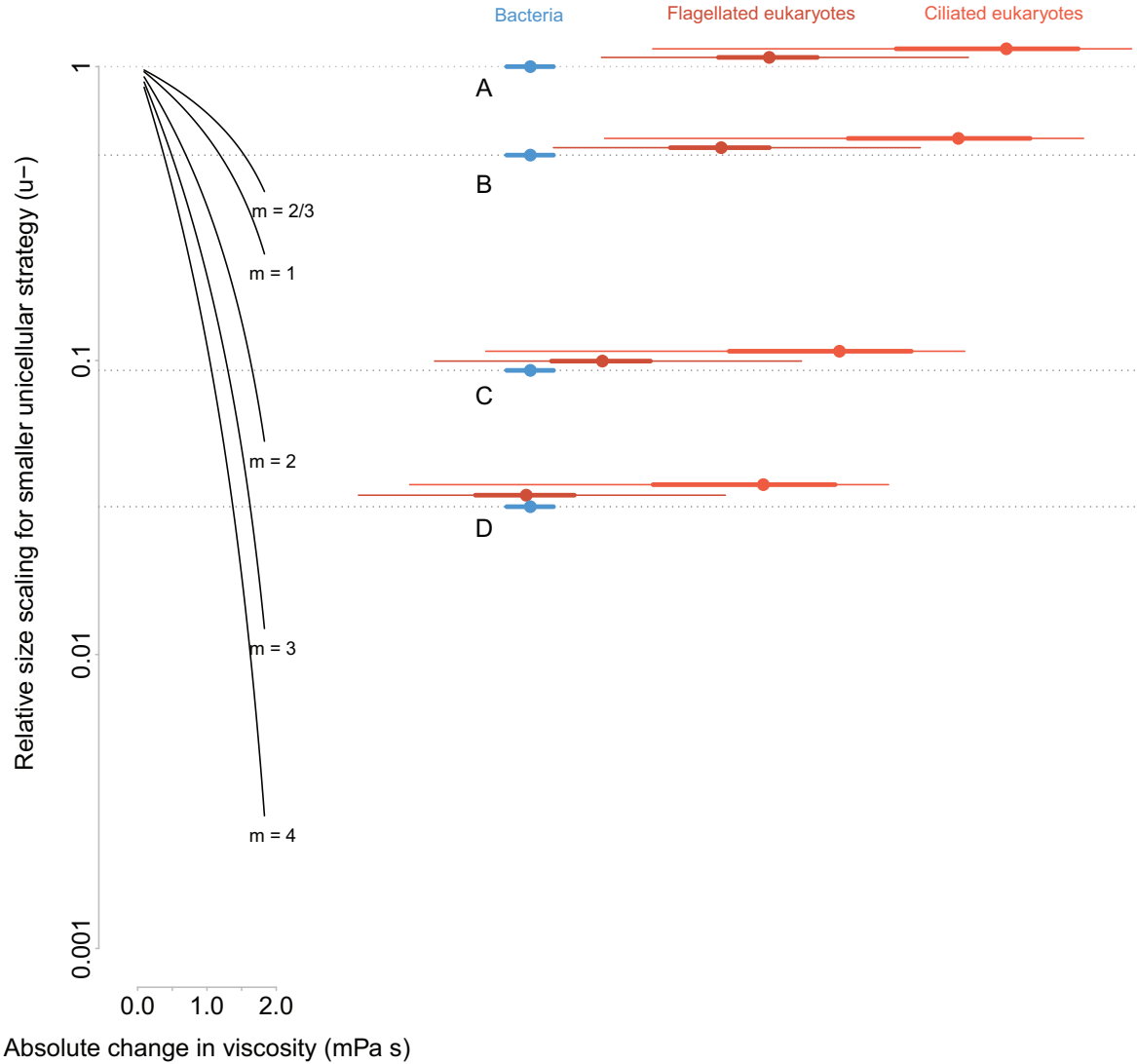
Figure 5: Consequences of evolving smaller unicellular (u−) size in response to increases in viscosity associated with the Snowball Earth glaciations. The magnitude of the size scaling involved in this strategy depends on the parameter *m*, the scaling between swimming velocity and viscosity. Evolving smaller cell size is a viable adaptive strategy from the point of view of nutrient balance; however, the sizes required to do so converge on the sizes of bacteria. *A*, Modern size distributions of bacteria, flagellated eukaryotes, and ciliated eukaryotes. Points denote median sizes, whereas thick lines denote interquartile ranges. *B*, Size scaling at which the smallest eukaryotes are the same size as the top quartile of bacteria. *C*, Size scaling at which the bottom quartile of eukaryotes are the same size as the top quartile of bacteria. *D*, Size scaling at which the median for flagellated eukaryotes would be the same size as the median size of bacteria. Competition with bacteria may prohibit eukaryotes from evolving this strategy.

Volvox-*like Multicellular Strategy (M1)*

The M1 strategy follows Solari et al. (2006) and features hollow colonies structured like *Volvox* with speeds that scale with the number of outer cells so that $v = N^{1/4}R^0\alpha\mu^{-m}$. Consequently, the encounter rate is $E = N^{1/4}\alpha\mu^{-m}C\pi R^2$, where $N = 4\pi R^2$ and the relative change in encounter rate is

$$\frac{E'}{E} = \left(\frac{R}{r}\right)^{1/2}\left(\frac{\mu'}{\mu}\right)^{-m}\left(\frac{R}{r}\right)^2. \qquad (11)$$

Because all cells are at the surface to make a blastula-like hollow sphere, the number of cells equals the surface area, assuming that cells fill that area. The relative change in the metabolic rate therefore is

$$\frac{M'}{M} = N\frac{r^3}{r^3} = \left(\frac{R}{r}\right)^2. \tag{12}$$

The nutrient balance for the M1 strategy is given by the ratio E'/M', which after simplifying is

$$\frac{E'}{M'} = \left(\frac{R}{r}\right)^{1/2}\left(\frac{\mu'}{\mu}\right)^{-m}. \tag{13}$$

The size needed to reach nutrient balance (where $E'/M' = 1$) occurs when

$$\frac{R}{r} = \left(\frac{\mu'}{\mu}\right)^{2m}. \tag{14}$$

The *Volvox*-like multicellular strategy has two advantages over the u+ strategy: a higher speed and a lower volume of metabolically active cells (figs. 3, 4). Increases in size and speeds beyond what is needed for nutrient balance are possible.

Spongelike Multicellular Strategy (M2)

For the M2 strategy, the relative speed of water through the organism scales with the volume of the organism (Morganti et al. 2019), so $N^b = 1$ and $R^a = R^{3 \times 0.6}$ in the template equation. The encounter rate for M2 is $E = (R/r)^{3 \times 0.6}\alpha\mu^{-m}C\pi R^2$, and the relative change in the encounter rate is

$$\frac{E'}{E} = \left(\frac{R}{r}\right)^{1.8}\left(\frac{\mu'}{\mu}\right)^{-m}\left(\frac{R}{r}\right)^2. \tag{15}$$

Because all cells are at the surface to make a hollow sphere, the number of cells equals the surface area, and the relative change in the metabolic rate is

$$\frac{M'}{M} = N = \left(\frac{R}{r}\right)^2. \tag{16}$$

The nutrient balance for M2 is given by the ratio E'/M', which after simplifying is

$$\frac{E'}{M'} = \left(\frac{R}{r}\right)^{1.8}\left(\frac{\mu'}{\mu}\right)^{-m}. \tag{17}$$

Nutrient balance ($E'/M' = 1$) occurs at the relative size change of

$$\frac{R}{r} = \left(\frac{\mu'}{\mu}\right)^{m/1.8}. \tag{18}$$

This spongelike multicellular strategy has an even higher relative speed than the M1 strategy, with a similarly low volume of metabolically active cells (figs. 3, 4). An organism with an M2 strategy is likely to be sessile so that it remains fixed with seawater actively moving through it. It is

interesting to note that for both M2 and M1, the speed that results in nutrient balance is equal to the speed of their unicellular ancestors. By increasing size and speeds beyond what is needed for nutrient balance, excess nutrients are accessible.

Slow Multicellular Strategy (M3)

For the M3 strategy, the relative swimming speed of the organism scales with the size of the organism (Solari et al. 2006, 2008; Lisicki et al. 2019; Montgomery et al. 2019), so $N^b = 1$ and $R^a = R^{0.6}$ in the template equation so that $v = R^{0.6}\alpha\mu^{-m}$. Consequently, the relative change in encounter rate is

$$\frac{E'}{E} = \left(\frac{R}{r}\right)^{0.6}\left(\frac{\mu'}{\mu}\right)^{-m}\left(\frac{R}{r}\right)^2. \tag{19}$$

In the M3 strategy, I assume that the full volume is filled with cells but the metabolic rate scales by volume to the three-fourths power ($\sim R^{9/4}$). This yields a relative change in metabolic rate of

$$\frac{M'}{M} = \left(\frac{R}{r}\right)^{9/4}. \tag{20}$$

The pattern nutrient balance for M3 is given by the ratio E'/M', which after simplifying is

$$\frac{E'}{M'} = \left(\frac{R}{r}\right)^{-0.35}\left(\frac{\mu'}{\mu}\right)^{-m}. \tag{21}$$

Nutrient balance ($E'/M' = 1$) occurs at the relative size change of

$$\frac{R}{r} = \left(\frac{\mu'}{\mu}\right)^{m/0.35}. \tag{22}$$

This multicellular strategy requires substantial size and speed increases to increase the encounter rate sufficiently for the full volume of metabolically active cells (figs. 3, 4). For the case of $m = 4$, the change in encounter rates is equivalent to the change in Reynolds numbers. Because of the sizes and speeds needed to reach nutrient balance, the organisms evolving by this strategy would increase their Reynolds numbers by about eight orders of magnitude.

Fast Multicellular Strategy (M4)

For the M4 strategy, the relative swimming speed of the organism scales with the size of the organism (Vogel 2008), so $a = 1$. In the template equation, speed is a function of colony radius rather than cell number, so that $v = R^1\alpha\mu^{-m}$. Consequently, the encounter rate is $E = \alpha\mu^{-m}C\pi R^3$, and the relative change in the encounter rate is

$$\frac{E'}{E} = \left(\frac{R}{r}\right)^1 \left(\frac{\mu'}{\mu}\right)^{-m} \left(\frac{R}{r}\right)^2. \qquad (23)$$

As with the M3 strategy, the full volume of M4 is filled with cells with a metabolic rate that scales by volume to the three-fourths power ($\sim R^{9/4}$):

$$\frac{M'}{M} = \left(\frac{R}{r}\right)^{9/4}. \qquad (24)$$

The pattern nutrient balance for M4 is given by the ratio E'/M', which after simplifying is

$$\frac{E'}{M'} = \left(\frac{R}{r}\right)^{3/4} \left(\frac{\mu'}{\mu}\right)^{-m}. \qquad (25)$$

Nutrient balance ($E'/M' = 1$) occurs at the relative size change of

$$\frac{R}{r} = \left(\frac{\mu'}{\mu}\right)^{4m/3}. \qquad (26)$$

The multicellular strategy M4 requires increases in size and speed so that the encounter rate is sufficient for the full volume of metabolically active cells (figs. 3, 4).

A Comparison of Adaptive Strategies

Each adaptive strategy is framed in terms of the rate of nutrient encounter relative to the rate of metabolic nutrient use. In all strategies, encounter rates are a function of size and speed, whereas metabolic rates are a function of size. Because surface area and therefore encounter rates scale more slowly than volume and metabolic rates, evolving a large unicellular strategy (u+) produces the largest metabolic deficit, worse even than no adaptation at all. Evolving smaller (u−), however, is a viable adaptive strategy. Smaller-sized cells have lower metabolic rates, and therefore it will always be possible to evolve small enough to eliminate metabolic deficits (fig. 4).

However, it is worth stepping back to understand what a decrease in size of this magnitude implies in terms of Péclet numbers and therefore feeding ecology. Even without factoring in whatever changes in motility must occur with such a decrease in size, the decrease in size alone would drop Pe by a factor of $(\mu/\mu')^m$, or 4^{-4} in the most extreme scenarios (fig. 5). This change in size moves the mean Pe for flagellated eukaryotes from $\overline{Pe} = 3.4$ to $\overline{Pe} = 0.028$ and therefore encroaches on the Pe range occupied by bacteria. Bacteria, being smaller and diffusion specialists, would likely outcompete any novel microeukaryote that would evolve extremes of this strategy. However, picoeukaryotes (<3 μm) are phylogenetically diverse (e.g., Rocke et al. 2013) and may, depending on the timing of their origins, represent a successful example of this strategy.

The scaling parameter m, which represents the scaling between viscosity and speed, has a large effect on the magnitude of the metabolic deficit introduced by high viscosity. But it has little effect on the qualitative relationships between viscosity and the adaptive strategies outlined here. There is, however, a special case where $m = 4$, where the relative change in the encounter rate is algebraically identical to tracking the relative change in the Reynolds number. As shown in figures 3 and 4, the encounter rates (and therefore the Reynolds numbers) for the points of nutrient balance for the four multicellular strategies increase by several orders of magnitude. The end result of these multicellular adaptive strategies is the evolution of high Reynolds numbers (Re $\gg 1$) from unicellular ancestors with low Reynolds numbers (Re $\ll 1$).

There is no doubt that the fluid physics approach I use here is overly simple. Yet a more complex stokeslet fluid dynamics approach to tracking flows made by small choanoflagellate colonies shows similar results, where colonial living provides a benefit to cells (Roper et al. 2013).

Modular cellular construction gives multicellular strategies advantages over unicellular strategies because of its effect on resource transport and the speeds multicellularity makes attainable. The scaling between metabolic rate and volume shifts from approximately 1 in unicellular eukaryotes to approximately three-fourths in metazoans (DeLong et al. 2010). Moreover, the higher flows that are possible by being a part of a larger and faster-moving cluster of cells helps individual cells gain relatively more nutrients than they could gather alone in high viscosity. Multicellular clusters can keep growing in size and increase their motility, and the individual cells within them benefit up to and even exceeding their metabolic needs (fig. 4). Moreover, Humphries (2009) has shown that at intermediate Reynolds numbers ($0.1 \leq$ Re ≤ 50), which the transition to multicellularity spans, encounter rates tend to be higher than expected because of compression of streamlines around objects or organisms. This enhancement of encounter rates at intermediate sizes would give an extra nutrient boost, beyond the encounter rates calculated here, to nascent multicellular organisms.

The Record of Multicellularity and Large Sizes

The cellular colonies or simple multicellular organisms observed in the Proterozoic fossil record prior to Snowball Earth are typically microscopic with few cells (Butterfield 2009; Cohen and Macdonald 2015; fig. 6). The multicellular clusters predicted by adaptation to the high viscosity of Snowball oceans may be many times larger than observed cellular colonies and posses an orders of magnitude or more cells ($R/r^2 \leq N \leq R/r^3$). At the extreme, the body sizes and cell numbers predicted by multicellular adaptive
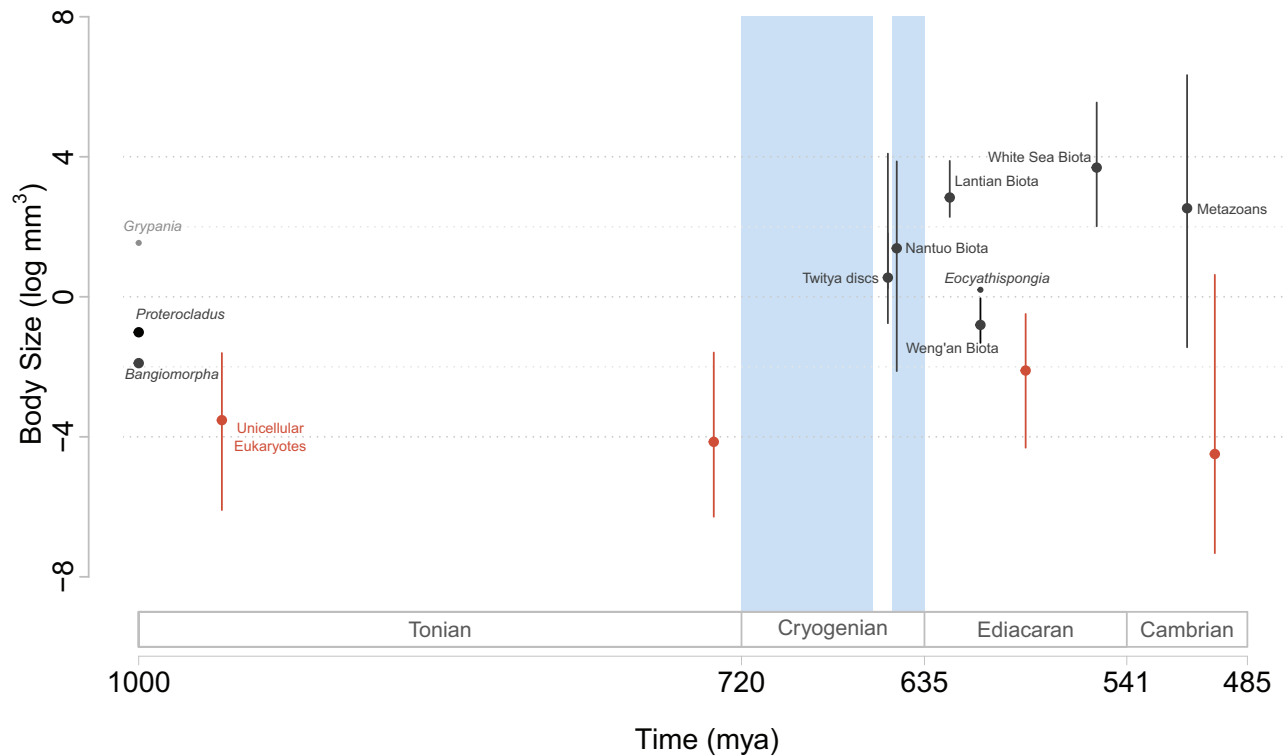
Figure 6: Observed fossil size distributions (log volume mm³) from the beginning of the Neoproterozoic (about 1,000 Ma) until the end of the Cambrian (485 Ma). Sturtian and Maranoan glaciations are shown in blue bands. Unicellular eukaryote fossils are shown in red. Multicellular forms are shown in black. Within the Cryogenian and Ediacaran, I show size distributions of biotas that include algal forms, metazoan forms, and forms with unknown affinity. The enigmatic *Grypania* is shown in gray because it is unlikely to be multicellular. mya = million years ago.

strategies span the gap between solitary eukaryotic unicellular organisms and the sizes and cell numbers characteristic of metazoans and macroalgae.

The existence of simple multicellular eukaryotes prior to the Snowball Earth (Butterfield 2009; Cohen and Macdonald 2015; Bykova et al. 2020) does not disprove the hypothesis that complex multicellularity results from an evolutionary response to increases in seawater viscosity. Variation in traits always arise independently from and before selection can act (Brandon 1990) because a lack of preexisting variation prevents evolution by natural selection (Fisher 1930). A preexisting ability to produce small and simple cellular clusters by adhesion of daughter cells and cell-to-cell signaling (King et al. 2003; Butterfield 2009; Sebé-Pedrós et al. 2017) is sufficient preexisting variation to permit multicellular adaptation toward much larger sizes and coordinate spatial organization in the presence of a new selective regime.

The rise of complex multicellularity in metazoans and the algal groups is different from what came before because these groups represent the first time that large size and multicellularity occur together (fig. 6). Early multicellular organisms, such as the 1.2-billion-year-old *Bangio-*

morpha (Butterfield 2000) and the 1-billion-year-old *Proterocladus* (Tang et al. 2020), are small compared with the very large sizes achieved by algae and early animals even in the midst of the Cryogenian (Cohen et al. 2015; Ye et al. 2015; Burzynski et al. 2020; fig. 6). Additionally, there are macroscopic fossils in the Proterozoic that predate the Snowball Earth glaciations by up to 1 billion years, such as *Grypania* (Hofmann 1985; fig. 6), but it is unlikely that these fossils represent multicellular organisms (Butterfield 2009, 2015; Anderson et al. 2020). A low diversity of simple macroscopic algae occurs prior to the Cryogenian, but their size and surface area–to–volume ratios expand dramatically in the Cryogenian and Ediacaran (Bykova et al. 2020).

After Glaciation

After Snowball Earth, oceans would have experienced a decrease in seawater viscosity when the glaciers melted and the oceans warmed, potentially dramatically (Yang et al. 2017). The ecological impact of warm seawater would have been significant for multicellular clusters with large absolute size and insignificant for multicellular clusters

or cells that were small. Even without subsequent adaptation, the encounter rates of multicellular eukaryotes would have increased substantially after deglaciation from the drop in viscosity alone, allowing further evolution of sizes as the colony became nutrient replete and able to maintain more cells. For some species, returning to a unicellular mode of life would no doubt be an evolutionary response to lower-viscosity oceans. Nevertheless, some multicellular eukaryotes would have been exposed to qualitatively novel flow regimes not previously accessible to their single-celled ancestors. As Reynolds numbers for multicellular eukaryotes increase, they leave viscous forces behind, and organisms can easily manipulate fluid flow directly. With this ability to interact with and manipulate flow granted by larger size, new ecologies are possible.

The Ediacaran fauna lived in a complex fluid environment (Ghisalberti et al. 2014; Rahman et al. 2015; Darroch et al. 2018; Gibson et al. 2021). Filter-feeding sponges are likely to have made their first appearance in the interlude between the Sturtian and Marinoan glaciations (Love et al. 2009, 2020; Maloof et al. 2010; Love and Summons 2015; Gold et al. 2016). Sponge larvae have Reynolds numbers near 1 (Woollacott 1990; Woollacott 1993), and a single sponge osculum can have Reynolds numbers that range from 17 to 150 (Goldstein et al. 2019). The individual choanocytes of sponges do not pump as much fluid as a solitary choanoflagellate (Larsen and Riisgård 1994; Nielsen et al. 2017; Asadzadeh et al. 2019); nevertheless, the choanocytes work together within the canals of a sponge, and massive flows can be produced, on the order of 200 L of water per hour (Leys et al. 2011; Leys and Kahn 2018).

The warm interlude after the Sturtian glaciation soon vanished as the Marinoan glaciation hit. Because of the effect of viscosity on cilia and flagella and the important role cilia and flagella play in physiology and behavior in unicellular and multicellular life (Larsen and Riisgård 2009; Humphries 2013), it is possible that complex multicellular organisms adapted to this second Snowball ocean by becoming larger yet to maintain or increase their encounter rates of nutrients. Although current data are sparse, figure 6 shows a second increase in the size of multicellular life after the Marinoan glaciation. The Gaskiers glaciation (579 Ma) is a third short and possibly global event that occurred in the Ediacaran and immediately predates the diverse, abundant, and large Ediacaran fauna (Pu et al. 2016; Darroch et al. 2018), shown as the White Sea biota in figure 6.

A Path to Complexity

Sizes and speeds of multicellular organisms may ratchet up across multiple global glaciations. Because of the large increase in cell numbers predicted by this viscosity mechanism, there are many physical consequences and physiological challenges that nascent multicellular organisms must overcome for this size ratchet to be successful. The solutions are the very features we associate with complex multicellularity: spatial organization and division of labor.

With large numbers of cells, geometric constraints arise that may lead to gastrulation, to orient flagellated surfaces on the outside of the body to help maintain motility (Buss 1987), and cellular differentiation, as internal cells are freed from motility requirements (Solari et al. 2006) and as gradients are formed inside the body (Schlichting 2003).

However, the evolution of traits such as these require an additional factor that acts to increase heritability at the level of the multicellular organism—a life cycle with a single-cell bottleneck (Grosberg and Strathmann 1998). A multicellular organism that develops from a single cell early in its life cycle is constructed from cells that stay together after cell division (Tarnita et al. 2013). The single-cell bottleneck acts to purge organisms of cheaters (Buss 1987; Grosberg and Strathmann 1998; Simpson 2011; Tarnita et al. 2013) and to increase the heritability of differentiated cell types (Simpson 2012). Some minor groups have aggregative multicellularity (Herron et al. 2013), but all examples of aggregative multicellularity originated on land (Bonner 1998; Fisher et al. 2020; Ostrowski 2020) and exhibit limited evolutionary potential (Pentz et al. 2020).

A morula-like embryo, filled with cells but lacking intercellular transport, cannot generate encounter rates sufficient to satisfy their metabolic needs—they act as a u+ strategy. Prior to gastrulation, cell division subdivides animal embryos, maintaining total volume but increasing cell number. The origin of maternal effects occurred phylogenetically early and spans this awkward stretch of development (Buss 1987).

Conclusions

The origin of metazoans and other groups with complex multicellularity during the Neoproterozoic transformed not only ecology but also the Earth system (Payne et al. 2020). The hypothesis presented here provides a mechanistic explanation for the concurrent origin of complex multicellularity in a number of independent lineages. However, this hypothesis is indeed challenging to test directly in the fossil record. The abrupt appearance of fossils in the Cryogenian that are many orders of magnitude larger than those earlier in the fossil record and a second increase in size postdating the Marinoan glaciation hints at a significant evolutionary role for Snowball Earth glaciations in the origin of complex multicellularity (fig. 6). Moreover, because oxygen is likely to have increased continuously over the Neoproterozoic (Cole et al. 2020) it is important

to note that the predicted colinear increase in body sizes is not observed. Rather, the largest increase in size occurs from the Tonian to the Cryogenian (fig. 6), suggesting that size increases are more tightly coupled to viscosity changes than to any rise in oxygen over this interval in time. More work on the macroevolution of Neoproterozoic body sizes is needed for a more conclusive test to distinguish between these two hypotheses.

Because multicellularity is evolvable in the laboratory (Ratcliff et al. 2012), the viscosity hypothesis is also easily tested using an experimental macroevolution approach (in the sense of Bell 2016). A quantitative prediction between the change in viscosity and a change in size is given by the equations presented above, conditioned on the specific scaling of motility and viscosity (fig. 4). Moreover, this viscosity hypothesis can be soundly rejected if multicellularity never experimentally evolves in high viscosity.

Even if seawater conditions change, an organism can maintain its physical interactions with the fluid by adapting its size and speed (Hutchinson 1967; Vogel 1996, 2008). And so complex multicellularity, through the large sizes and high motility it makes possible, can provide a fluid dynamic refuge from the ubiquitous high viscosity of Snowball oceans.

There are, in fact, hints that adaptation to high-viscosity seawater is important today. Many marine eukaryotes that live in cold conditions tend to more often be colonial forms or larger than lower-latitude unicellular organisms (Barton et al. 2013; Sommer et al. 2017). Relatively larger cold water morphs also are detectable in the fossil record (e.g., Mousing et al. 2017). When grown in high-viscosity media, the unicellular eukaryote *Chlamydomonas* tends to form clusters (Lewin 1954). Many phytoplankton exhibit putative multicellular attributes (Abada and Segev 2018). For example, the haptophyte algal genus *Phaeocystis* has multicellular forms that tend to occur in colder polar oceans, whereas the unicellular forms occur in warmer temperate oceans (Beardall et al. 2009). Many of the phenotypic changes associated with cold and viscous conditions are seasonally plastic (cyclomorphosis) and include increased cell size and increases in cell number in colonies (Trainor 1993; Zohary et al. 2017; Zohary et al. 2020).

During the Cryogenian, any whiff of latitudinal gradients and seasonality was surely lost with the accumulation of sea ice and the associated drop in productivity. Every new species for the 70 million years of Cryogenian glaciation originated in cold conditions, likely with severe resource limitations. To the extent that macroevolution involves the maximization of energy control (e.g., Van Valen 1976), in the context of the Snowball Earth the ecological advantages available at higher Reynolds numbers (accessible only to those with large size and high speed) would have been profound. The high viscosity of cold sea-

water during Snowball Earth would have knocked warm-adapted unicellular species off their adaptive peak with a clear path to start climbing back up to a new and even higher peak.

Cold, high-viscosity environments similar to those during the Neoproterozoic glaciations are common on the Earth today at the poles and in the deep sea. These environments would have also been common over the Phanerozoic during ice house intervals as well as prior to the Neoproterozoic glaciations, such as during the Paleoproterozoic Huronian glaciation that occurred 2.4–2.1 billion years ago (Kopp et al. 2005). Yet the origins of new multicellular groups did not occur until the Neoproterozoic, and their origins have also been a rare occurrence after the Neoproterozoic (Herron et al. 2009; Knoll 2011). Although the Paleoproterozoic, Neoproterozoic, and Phanerozoic glacial environments are physically similar, they are each strikingly different ecologically. The Huronian glaciation occurred prior to the origin of eukaryotes (Cohen and Macdonald 2015). As bacterial ecologies are dominated by diffusion, bacteria would have been able to adapt to high-viscosity environments by decreasing their size proportional to the decline in diffusivity. Animals and macroalgae dominate marine environments during Phanerozoic ice houses (including today), so any multicellular organisms evolving then would have faced intense competition for resources. Multicellular eukaryotes originating during the Neoproterozic glaciations would be radiating into a wholly unoccupied resource space.

The evolutionary significance of the Snowball Earth glaciations is not just in the extremity of the environments but in the combination of the long-term (70 million years) loss of important temperate and tropical shallow-water habitats with the presence of a wholly unoccupied ecospace. The confluence of both physical homogeneity and ecological opportunity was geologically unique.

The sizes and speeds that are possible with multicellular bodies permit life to escape viscous forces and to live and swim in a new ocean, one that was always there but just out of reach.

Acknowledgments

Data and Code Availability

Literature Cited

Abada, A., and E. Segev. 2018. Multicellular features of phytoplankton. Frontiers in Marine Science 5:144.

Abbot, D. S., A. Voigt, and D. Koll. 2011. The Jormungand global climate state and implications for Neoproterozoic glaciations. Journal of Geophysical Research: Atmospheres 116:D18103.

Ajani, P. A., N. McGinty, Z. V. Finkel, and A. J. Irwin. 2018. Phytoplankton realized niches track changing oceanic conditions at a long-term coastal station off Sydney Australia. Frontiers in Marine Science 5:285.

Anderson, R. P., N. J. Tosca, G. Cinque, M. D. Frogley, I. Lekkas, A. Akey, G. M. Hughes, et al. 2020. Aluminosilicate haloes preserve complex life approximately 800 million years ago. Interface Focus 10:20200011.

Asadzadeh, S. S., P. S. Larsen, H. U. Riisgård, and J. H. Walther. 2019. Hydrodynamics of the leucon sponge pump. Journal of the Royal Society Interface 16:20180630.

Ashkenazy, Y., H. Gildor, M. Losch, F. A. Macdonald, D. P. Schrag, and E. Tziperman. 2013. Dynamics of a Snowball Earth ocean. Nature 495:90–93.

Bambach, R. K., A. M. Bush, and D. H. Erwin. 2007. Autecology and the filling of ecospace: key metazoan radiations. Palaeontology 50:1–22.

Barton, A. D., A. J. Pershing, E. Litchman, N. R. Record, K. F. Edwards, Z. V. Finkel, T. Kiørboe, et al. 2013. The biogeography of marine plankton traits. Ecology Letters 16:522–534.

Beardall, J., D. Allen, J. Bragg, Z. V. Finkel, K. J. Flynn, A. Quigg, T. A. V. Rees, et al. 2009. Allometry and stoichiometry of unicellular, colonial and multicellular phytoplankton. New Phytologist 181:295–309.

Bell, G. 2016. Experimental macroevolution. Proceedings of the Royal Society B 283:20152547.

Blake, J. R., and M. A. Sleigh. 1974. Mechanics of ciliary locomotion. Biological Reviews 49:85–125.

Bonner, J. T. 1998. The origins of multicellularity. Integrative Biology: Issues, News, and Reviews 1:27–36.

———. 2001. First signals: the evolution of multicellular development. Princeton University Press, Princeton, NJ.

Bozdag, G. O., E. Libby, R. Pineau, C. T. Reinhard, and W. C. Ratcliff. 2021. Oxygen suppression of macroscopic multicellularity. Nature Communications 12:2838.

Branco, P., M. Egas, S. R. Hall, and J. Huisman. 2020. Why do phytoplankton evolve large size in response to grazing? American Naturalist 195:E20–E37.

Brandon, R. N. 1990. Adaptation and environment. Princeton University Press, Princeton, NJ.

Brocks, J. J., A. J. Jarrett, E. Sirantoine, C. Hallmann, Y. Hoshino, and T. Liyanage. 2017. The rise of algae in Cryogenian oceans and the emergence of animals. Nature 548:578–581.

Budd, G. E., and S. Jensen. 2017. The origin of the animals and a 'Savannah' hypothesis for early bilaterian evolution. Biological Reviews 92:446–473.

Burzynski, G., T. A. Dececchi, G. M. Narbonne, and R. W. Dalrymple. 2020. Cryogenian *Aspidella* from northwestern Canada. Precambrian Research 336:105507.

Buss, L. W. 1987. The evolution of individuality. Princeton University Press, Princeton, NJ.

Butterfield, N. J. 2000. *Bangiomorpha pubescens* n. gen., n. sp.: implications for the evolution of sex, multicellularity, and the Mesoproterozoic/Neoproterozoic radiation of eukaryotes. Paleobiology 26:386–404.

———. 2009. Modes of pre-Ediacaran multicellularity. Precambrian Research 173:201–211.

———. 2011. Animals and the invention of the Phanerozoic Earth system. Trends in Ecology and Evolution 26:81–87.

———. 2015. Proterozoic photosynthesis—a critical review. Palaeontology 58:953–972.

———. 2018. Oxygen, animals and aquatic bioturbation: an updated account. Geobiology 16:3–16.

Bykova, N., S. T. LoDuca, Q. Ye, V. Marusin, D. Grazhdankin, and S. Xiao. 2020. Seaweeds through time: morphological and ecological analysis of Proterozoic and early Paleozoic benthic macroalgae. Precambrian Research 350:105875.

Canfield, D. E., and J. Farquhar. 2009. Animal evolution, bioturbation, and the sulfate concentration of the oceans. Proceedings of the National Academy of Sciences of the USA 106:8123–8127.

Cloud, P. 1976. Beginnings of biospheric evolution and their biogeochemical consequences. Paleobiology 2:351–387.

Cohen, P. A., and F. A. Macdonald. 2015. The Proterozoic record of eukaryotes. Paleobiology 41:610–632.

Cohen, P. A., F. A. Macdonald, S. Pruss, E. Matys, and T. Bosak. 2015. Fossils of putative marine algae from the Cryogenian glacial interlude of Mongolia. Palaios 30:238–247.

Cohen, P. A., and L. A. Riedman. 2018. It's a protist-eat-protist world: recalcitrance, predation, and evolution in the Tonian-Cryogenian ocean. Emerging Topics in Life Sciences 28:173–180.

Cohen, P. A., J. W. Schopf, N. J. Butterfield, A. B. Kudryavtsev, and F. A. Macdonald. 2011. Phosphate biomineralization in mid-Neoproterozoic protists. Geology 39:539–542.

Cohen, P. A., M. Vizcaíno, and R. P. Anderson. 2020. Oldest fossil ciliates from the Cryogenian glacial interlude reinterpreted as possible red algal spores. Palaeontology 63:941–950.

Cole, D. B., D. B. Mills, D. H. Erwin, E. A. Sperling, S. M. Porter, C. T. Reinhard, and N. J. Planavsky. 2020. On the co-evolution of surface oxygen levels and animals. Geobiology 18:260–281.

Colin, S. P., J. H. Costello, K. R. Sutherland, B. J. Gemmell, J. O. Dabiri, and K. T. Du Clos. 2020. The role of suction thrust in the metachronal paddles of swimming invertebrates. Scientific Reports 10:1–8.

Corsetti, F. A., A. N. Olcott, and C. Bakermans. 2006. The biotic response to Neoproterozoic snowball Earth. Palaeogeography, Palaeoclimatology, Palaeoecology 232:114–130.

Darroch, S. A., M. Laflamme, and P. J. Wagner. 2018. High ecological complexity in benthic Ediacaran communities. Nature Ecology and Evolution 2:1541–1547.

De Goeij, J. M., D. Van Oevelen, M. J. Vermeij, R. Osinga, J. J. Middelburg, A. F. De Goeij, and W. Admiraal. 2013. Surviving in a marine desert: the sponge loop retains resources within coral reefs. Science 342:108–110.

Del Cortona, A., C. J. Jackson, F. Bucchini, M. Van Bel, S. D'hondt, P. Škaloud, C. F. Delwiche, et al. 2020. Neoproterozoic origin

and multiple transitions to macroscopic growth in green seaweeds. Proceedings of the National Academy of Sciences of the USA 117:2551–2559.

DeLong, J. P., J. G. Okie, M. E. Moses, R. M. Sibly, and J. H. Brown. 2010. Shifts in metabolic scaling, production, and efficiency across major evolutionary transitions of life. Proceedings of the National Academy of Sciences of the USA 107:12941–12945.

Dombrowski, T., S. K. Jones, G. Katsikis, A. P. S. Bhalla, B. E. Griffith, and D. Klotsa. 2019. Transition in swimming direction in a model self-propelled inertial swimmer. Physical Review Fluids 4:021101.

Dorsey, N. 1968. Properties of ordinary water-substance. Hafner, New York.

dos Reis, M., Y. Thawornwattana, K. Angelis, M. J. Telford, P. C. Donoghue, and Z. Yang. 2015. Uncertainty in the timing of origin of animals and the limits of precision in molecular timescales. Current Biology 25:2939–2950.

Erwin, D. H., M. Laflamme, S. M. Tweedt, E. A. Sperling, D. Pisani, and K. J. Peterson. 2011. The Cambrian conundrum: early divergence and later ecological success in the early history of animals. Science 334:1091–1097.

Fenchel, T. 1987. Ecology of protozoa: the biology of free-living phagotropic protists. Springer, Berlin.

Fernandes, N. M., and C. G. Schrago. 2019. A multigene timescale and diversification dynamics of Ciliophora evolution. Molecular Phylogenetics and Evolution 139:106521.

Fiorella, R. P., and N. D. Sheldon. 2017. Equable end Mesoproterozoic climate in the absence of high CO_2. Geology 45:231–234.

Fisher, R. A. 1930. The genetical theory of natural selection: a complete variorum edition. Oxford University Press, Oxford.

Fisher, R. M., J. Z. Shik, and J. J. Boomsma. 2020. The evolution of multicellular complexity: the role of relatedness and environmental constraints. Proceedings of the Royal Society B 287:20192963.

Gheber, L., A. Korngreen, and Z. Priel. 1998. Effect of viscosity on metachrony in mucus propelling cilia. Cell Motility and the Cytoskeleton 39:9–20.

Ghisalberti, M., D. A. Gold, M. Laflamme, M. E. Clapham, G. M. Narbonne, R. E. Summons, D. T. Johnston, et al. 2014. Canopy flow analysis reveals the advantage of size in the oldest communities of multicellular eukaryotes. Current Biology 24:305–309.

Gibson, B. M., D. J. Furbish, I. A. Rahman, M. W. Schmeeckle, M. Laflamme, and S. A. Darroch. 2021. Ancient life and moving fluids. Biological Reviews 96:129–152.

Gold, D. A., J. Grabenstatter, A. De Mendoza, A. Riesgo, I. Ruiz-Trillo, and R. E. Summons. 2016. Sterol and genomic analyses validate the sponge biomarker hypothesis. Proceedings of the National Academy of Sciences of the USA 113:2684–2689.

Goldstein, J., H. U. Riisgård, and P. S. Larsen. 2019. Exhalant jet speed of single-osculum explants of the demosponge *Halichondria panicea* and basic properties of the sponge-pump. Journal of Experimental Marine Biology and Ecology 511:82–90.

Goldstein, R. E. 2015. Green algae as model organisms for biological fluid dynamics. Annual Review of Fluid Mechanics 47:343–375.

Grosberg, R. K., and R. R. Strathmann. 1998. One cell, two cell, red cell, blue cell: the persistence of a unicellular stage in multicellular life histories. Trends in Ecology and Evolution 13:112–116.

———. 2007. The evolution of multicellularity: a minor major transition? Annual Review of Ecology, Evolution, and Systematics 38:621–654.

Guasto, J. S., R. Rusconi, and R. Stocker. 2012. Fluid mechanics of planktonic microorganisms. Annual Review of Fluid Mechanics 44:373–400.

Heim, N. A., J. L. Payne, S. Finnegan, M. L. Knope, M. Kowalewski, S. K. Lyons, D. W. McShea, et al. 2017. Hierarchical complexity and the size limits of life. Proceedings of the Royal Society B 284:20171039.

Herron, M. D., J. M. Borin, J. C. Boswell, J. Walker, I.-C. K. Chen, C. A. Knox, M. Boyd, et al. 2019. De novo origins of multicellularity in response to predation. Scientific Reports 9:2328.

Herron, M. D., J. D. Hackett, F. O. Aylward, and R. E. Michod. 2009. Triassic origin and early radiation of multicellular volvocine algae. Proceedings of the National Academy of Sciences of the USA 106:3254–3258.

Herron, M. D., A. Rashidi, D. E. Shelton, and W. W. Driscoll. 2013. Cellular differentiation and individuality in the "minor" multicellular taxa. Biological Reviews 88:844–861.

Hoffman, P. F., D. S. Abbot, Y. Ashkenazy, D. I. Benn, J. J. Brocks, P. A. Cohen, G. M. Cox, et al. 2017. Snowball Earth climate dynamics and Cryogenian geology geobiology. Science Advances 3:e1600983.

Hoffman, P. F., A. J. Kaufman, G. P. Halverson, and D. P. Schrag. 1998. A Neoproterozoic snowball earth. Science 281:1342–1346.

Hofmann, H. J. 1985. Precambrian carbonaceous megafossils. Pages 20–33 in Paleoalgology. Springer, Berlin.

Hofmann, H., G. Narbonne, and J. Aitken. 1990. Ediacaran remains from intertillite beds in northwestern Canada. Geology 18:1199–1202.

Humphries, S. 2009. Filter feeders and plankton increase particle encounter rates through flow regime control. Proceedings of the National Academy of Sciences of the USA 106:7882–7887.

———. 2013. A physical explanation of the temperature dependence of physiological processes mediated by cilia and flagella. Proceedings of the National Academy of Sciences of the USA 110:14693–14698.

Hutchinson, G. E. 1967. A treatise on limnology. Introduction *to* Lake biology and the limnoplankton. Vol. 2. Wiley, Hoboken, NJ.

Javaux, E. 2011. Early eukaryotes in Precambrian oceans. Pages 414–449 in M. Gargaud et al., eds. Origins and evolution of life: an astrobiological perspective. Cambridge University Press, Cambridge.

Kearns, D. B. 2010. A field guide to bacterial swarming motility. Nature Reviews Microbiology 8:634–644.

King, N., C. T. Hittinger, and S. B. Carroll. 2003. Evolution of key cell signaling and adhesion protein families predates animal origins. Science 301:361–363.

Kiørboe, T. 2011. How zooplankton feed: mechanisms, traits and trade-offs. Biological Reviews 86:311–339.

Kirschvink, J. L. 1992. Late Proterozoic low-latitude global glaciation: the snowball Earth. Pages 51–52 in The Proterozoic biosphere: a multidisciplinary study. Cambridge University Press, New York.

Klotsa, D., K. A. Baldwin, R. J. Hill, R. M. Bowley, and M. R. Swift. 2015. Propulsion of a two-sphere swimmer. Physical Review Letters 115:248102.

Knoll, A. H. 2011. The multiple origins of complex multicellularity. Annual Review of Earth and Planetary Sciences 39:217–239.

Knoll, A. H., and S. B. Carroll. 1999. Early animal evolution: emerging views from comparative biology and geology. Science 284:2129–2137.

Knoll, A. H., and D. Hewitt. 2011. Phylogenetic, functional and geological perspectives on complex multicellularity. Pages 251–270 *in* The major transitions in evolution revisited. MIT Press, Cambridge, MA.

Knoll, A. H., and E. A. Sperling. 2014. Oxygen and animals in Earth history. Proceedings of the National Academy of Sciences of the USA 111:3907–3908.

Kopp, R. E., J. L. Kirschvink, I. A. Hilburn, and C. Z. Nash. 2005. The Paleoproterozoic snowball Earth: a climate disaster triggered by the evolution of oxygenic photosynthesis. Proceedings of the National Academy of Sciences of the USA 102:11131–11136.

LaBarbera, M. 1978. Precambrian geological history and the origin of the Metazoa. Nature 273:22–25.

Larsen, P. S., and H. U. Riisgård. 1994. The sponge pump. Journal of Theoretical Biology 168:53–63.

———. 2009. Viscosity and not biological mechanisms often controls the effects of temperature on ciliary activity and swimming velocity of small aquatic organisms. Journal of Experimental Marine Biology and Ecology 381:67–73.

Lenton, T. M., R. A. Boyle, S. W. Poulton, G. A. Shields-Zhou, and N. J. Butterfield. 2014. Co-evolution of eukaryotes and ocean oxygenation in the Neoproterozoic era. Nature Geoscience 7:257–265.

Lewin, R. A. 1954. Mutants of *Chlamydomonas moewusii* with impaired motility. Journal of General Microbiology 11:358–363.

Leys, S. P., and A. S. Kahn. 2018. Oxygen and the energetic requirements of the first multicellular animals. Integrative and Comparative Biology 58:666–676.

Leys, S. P., G. Yahel, M. A. Reidenbach, V. Tunnicliffe, U. Shavit, and H. M. Reiswig. 2011. The sponge pump: the role of current induced flow in the design of the sponge body plan. PLoS ONE 6:e27787.

Lisicki, M., M. F. Velho Rodrigues, R. E. Goldstein, and E. Lauga. 2019. Swimming eukaryotic microorganisms exhibit a universal speed distribution. eLife 8:e44907.

Liu, A. G., C. G. Kenchington, and E. G. Mitchell. 2015. Remarkable insights into the paleoecology of the Avalonian Ediacaran macrobiota. Gondwana Research 27:1355–1380.

Love, G. D., E. Grosjean, C. Stalvies, D. A. Fike, J. P. Grotzinger, A. S. Bradley, A. E. Kelly, et al. 2009. Fossil steroids record the appearance of Demospongiae during the Cryogenian period. Nature 457:718–721.

Love, G. D., and R. E. Summons. 2015. The molecular record of Cryogenian sponges—a response to Antcliffe (2013). Palaeontology 58:1131–1136.

Love, G. D., J. A. Zumberge, P. Cárdenas, E. A. Sperling, M. Rohrssen, E. Grosjean, J. P. Grotzinger, et al. 2020. Sources of C30 steroid biomarkers in Neoproterozoic—Cambrian rocks and oils. Nature Ecology and Evolution 4:34–36.

Macdonald, F. A., M. D. Schmitz, J. L. Crowley, C. F. Roots, D. S. Jones, A. C. Maloof, J. V. Strauss, et al. 2010. Calibrating the Cryogenian. Science 327:1241–1243.

MacLennan, S. A., M. P. Eddy, A. J. Merschat, A. K. Mehra, P. W. Crockford, A. C. Maloof, C. S. Southworth, et al. 2020. Geologic evidence for an icehouse Earth before the Sturtian global glaciation. Science Advances 6:eaay6647.

Maloof, A. C., C. V. Rose, R. Beach, B. M. Samuels, C. C. Calmet, D. H. Erwin, G. R. Poirier, et al. 2010. Possible animal-body fossils in pre-Marinoan limestones from South Australia. Nature Geoscience 3:653–659.

Mentel, M., M. Röttger, S. Leys, A. G. Tielens, and W. F. Martin. 2014. Of early animals, anaerobic mitochondria, and a modern sponge. BioEssays 36:924–932.

Mills, D. B. 2020. The origin of phagocytosis in Earth history. Interface Focus 10:20200019.

Mills, D. B., and D. E. Canfield. 2014. Oxygen and animal evolution: did a rise of atmospheric oxygen "trigger" the origin of animals? BioEssays 36:1145–1155.

Mills, D. B., W. R. Francis, S. Vargas, M. Larsen, C. P. H. Elemans, D. E. Canfield, and G. Wörheide. 2018. The last common ancestor of animals lacked the HIF pathway and respired in low-oxygen environments. eLife 7:e31176.

Mills, D. B., L. M. Ward, C. Jones, B. Sweeten, M. Forth, A. H. Treusch, and D. E. Canfield. 2014. Oxygen requirements of the earliest animals. Proceedings of the National Academy of Sciences of the USA 111:4168–4172.

Moczydłowska, M. 2008. The Ediacaran microbiota and the survival of Snowball Earth conditions. Precambrian Research 167:1–15.

Montgomery, E., J.-F. Hamel, and A. Mercier. 2019. Larval nutritional mode and swimming behaviour in ciliated marine larvae. Journal of the Marine Biological Association of the United Kingdom 99:1027–1032.

Morganti, T. M., M. Ribes, G. Yahel, and R. Coma. 2019. Size is the major determinant of pumping rates in marine sponges. Frontiers in Physiology 10:1474.

Mousing, E. A., S. Ribeiro, C. Chisholm, A. Kuijpers, M. Moros, and M. Ellegaard. 2017. Size differences of Arctic marine protists between two climate periods—using the paleoecological record to assess the importance of within-species trait variation. Ecology and Evolution 7:3–13.

Narbonne, G. M. 1994. New Ediacaran fossils from the Mackenzie Mountains, northwestern Canada. Journal of Paleontology 68:411–416.

Nayar, K. G., M. H. Sharqawy, and L. D. Banchik. 2016. Thermophysical properties of seawater: a review and new correlations that include pressure dependence. Desalination 390:1–24.

Nielsen, L. T., S. S. Asadzadeh, J. Dölger, J. H. Walther, T. Kiørboe, and A. Andersen. 2017. Hydrodynamics of microbial filter feeding. Proceedings of the National Academy of Sciences of the USA 114:9373–9378.

Niklas, K. J., and S. A. Newman. 2013. The origins of multicellular organisms. Evolution and Development 15:41–52.

Nursall, J. 1959. Oxygen as a prerequisite to the origin of the Metazoa. Nature 183:1170–1772.

Ostrowski, E. A. 2020. Evolution of multicellularity: one from many or many from one? Current Biology 30:R1306–R1308.

Payne, J. L., A. Bachan, N. A. Heim, P. M. Hull, and M. L. Knope. 2020. The evolution of complex life and the stabilization of the Earth system. Interface Focus 10:20190106.

Pentz, J. T., P. Márquez-Zacarías, G. O. Bozdag, A. Burnetti, P. J. Yunker, E. Libby, and W. C. Ratcliff. 2020. Ecological advantages and evolutionary limitations of aggregative multicellular development. Current Biology 30:4155–4164.

Pierrehumbert, R., D. Abbot, A. Voigt, and D. Koll. 2011. Climate of the Neoproterozoic. Annual Review of Earth and Planetary Sciences 39:417–460.

Podolsky, R. D. 1994. Temperature and water viscosity: physiological versus mechanical effects on suspension feeding. Science 265:100–103.

Podolsky, R. D., and R. B. Emlet. 1993. Separating the effects of temperature and viscosity on swimming and water movement by sand dollar larvae (*Dendraster excentricus*). Journal of Experimental Biology 176:207–222.

Porter, S. 2011. The rise of predators. Geology 39:607–608.

———. 2016. Tiny vampires in ancient seas: evidence for predation via perforation in fossils from the 780–740 million-year-old Chuar Group, Grand Canyon, USA. Proceedings of the Royal Society B: Biological Sciences 283:20160221.

Porter, S. M., R. Meisterfeld, and A. H. Knoll. 2003. Vase-shaped microfossils from the Neoproterozoic Chuar Group, Grand Canyon: a classification guided by modern testate amoebae. Journal of Paleontology 77:409–429.

Pu, J. P., S. A. Bowring, J. Ramezani, P. Myrow, T. D. Raub, E. Landing, A. Mills, et al. 2016. Dodging snowballs: geochronology of the Gaskiers glaciation and the first appearance of the Ediacaran biota. Geology 44:955–958.

Purcell, E. M. 1977. Life at low Reynolds number. American Journal of Physics 45:3–11.

Qin, B., A. Gopinath, J. Yang, J. P. Gollub, and P. E. Arratia. 2015. Flagellar kinematics and swimming of algal cells in viscoelastic fluids. Scientific Reports 5:9190.

Raff, R. A., and E. C. Raff. 1970. Respiratory mechanisms and the metazoan fossil record. Nature 228:1003–1005.

Rahman, I. A., S. A. Darroch, R. A. Racicot, and M. Laflamme. 2015. Suspension feeding in the enigmatic Ediacaran organism *Tribrachidium* demonstrates complexity of Neoproterozoic ecosystems. Science Advances 1:e1500800.

Ratcliff, W. C., R. F. Denison, M. Borrello, and M. Travisano. 2012. Experimental evolution of multicellularity. Proceedings of the National Academy of Sciences of the USA 109:1595–1600.

Rhoads, D. C., and J. W. Morse. 1971. Evolutionary and ecologic significance of oxygen-deficient marine basins. Lethaia 4:413–428.

Riedman, L. A., S. M. Porter, G. P. Halverson, M. T. Hurtgen, and C. K. Junium. 2014. Organic-walled microfossil assemblages from glacial and interglacial Neoproterozoic units of Australia and Svalbard. Geology 42:1011–1014.

Riedman, L. A., and P. M. Sadler. 2018. Global species richness record and biostratigraphic potential of early to middle Neoproterozoic eukaryote fossils. Precambrian Research 319:6–18.

Rocke, E., H. Jing, and H. Liu. 2013. Phylogenetic composition and distribution of picoeukaryotes in the hypoxic northwestern coast of the Gulf of Mexico. Microbiologyopen 2:130–143.

Roper, M., M. J. Dayel, R. E. Pepper, and M. Koehl. 2013. Cooperatively generated stresslet flows supply fresh fluid to multicellular choanoflagellate colonies. Physical Review Letters 110: 228104.

Schlichting, C. D. 2003. Origins of differentiation via phenotypic plasticity. Evolution and Development 5:98–105.

Sebé-Pedrós, A., B. M. Degnan, and I. Ruiz-Trillo. 2017. The origin of Metazoa: a unicellular perspective. Nature Reviews Genetics 18:498–512.

Sharqawy, M. H., J. H. Lienhard, and S. M. Zubair. 2010. Thermophysical properties of seawater: a review of existing correlations and data. Desalination and Water Treatment 16:354–380.

Simpson, C. 2011. How many levels are there? how insights from evolutionary transitions in individuality help measure the hierarchical complexity of life. Pages 199–226 *in* B. Calcott and K.

Sterelney, eds. The major transitions in evolution revisited. MIT Press, Cambridge, MA.

———. 2012. The evolutionary history of division of labour. Proceedings of the Royal Society B 279:116–121.

———. 2020. Data from: Adaptation to a viscous Snowball Earth ocean as a path to complex multicellularity. American Naturalist, Dryad Digital Repository, https://doi.org/10.5061/dryad.f1vhhmgvj.

Sleigh, M., and J. Blake. 1977. Method of ciliary production and their size limitations. Pages 243–256 *in* T. Pedley, ed. Scale effects in animal locomotion. Academic Press, London.

Solari, C. A., J. O. Kessler, and R. E. Michod. 2006. A hydrodynamics approach to the evolution of multicellularity: flagellar motility and germ-soma differentiation in volvocalean green algae. American Naturalist 167:537–554.

Solari, C. A., R. E. Michod, and R. E. Goldstein. 2008. *Volvox barberi*, the fastest swimmer of the Volvocales (Chlorophyceae). Journal of Phycology 44:1395–1398.

Sommer, U., K. H. Peter, S. Genitsaris, and M. Moustaka-Gouni. 2017. Do marine phytoplankton follow Bergmann's rule sensu lato? Biological Reviews 92:1011–1026.

Sperling, E. A., C. Carbone, J. V. Strauss, D. T. Johnston, G. M. Narbonne, and F. A. Macdonald. 2016. Oxygen, facies, and secular controls on the appearance of Cryogenian and Ediacaran body and trace fossils in the Mackenzie Mountains of northwestern Canada. Bulletin 128:558–575.

Sperling, E. A., C. A. Frieder, A. V. Raman, P. R. Girguis, L. A. Levin, and A. H. Knoll. 2013. Oxygen, ecology, and the Cambrian radiation of animals. Proceedings of the National Academy of Sciences of the USA 110:13446–13451.

Sperling, E. A., C. J. Wolock, A. S. Morgan, B. C. Gill, M. Kunzmann, G. P. Halverson, F. A. Macdonald, et al. 2015. Statistical analysis of iron geochemical data suggests limited late Proterozoic oxygenation. Nature 523:451–454.

Stanley, S. M. 1973. An ecological theory for the sudden origin of multicellular life in the late Precambrian. Proceedings of the National Academy of Sciences of the USA 70:1486–1489.

Tang, Q., K. Pang, X. Yuan, and S. Xiao. 2020. A one-billion-year-old multicellular chlorophyte. Nature Ecology and Evolution 4:543–549.

Tarnita, C. E., C. H. Taubes, and M. A. Nowak. 2013. Evolutionary construction by staying together and coming together. Journal of Theoretical Biology 320:10–22.

Towe, K. M. 1970. Oxygen-collagen priority and the early metazoan fossil record. Proceedings of the National Academy of Sciences of the USA 65:781–788.

Trainor, F. 1993. Cyclomorphosis in *Scenedesmus subspicatus* R. Chod. Cell behavior during the unicell-colony transformation of a phenotypicly plastic organism. Archiv für Protistenkunde 143:55–61.

Trower, E. J. 2020. The enigma of Neoproterozoic giant ooids—fingerprints of extreme climate? Geophysical Research Letters 47:e2019GL086146.

Trower, E. J., and J. P. Grotzinger. 2010. Sedimentology, diagenesis, and stratigraphic occurrence of giant ooids in the Ediacaran Rainstorm Member, Johnnie Formation, Death Valley region, California. Precambrian Research 180:113–124.

Trower, E. J., M. P. Lamb, and W. W. Fischer. 2017. Experimental evidence that ooid size reflects a dynamic equilibrium between rapid precipitation and abrasion rates. Earth and Planetary Science Letters 468:112–118.

Valentine, J. W., S. M. Awramik, P. W. Signor, and P. M. Sadler. 1991. The biological explosion at the Precambrian-Cambrian boundary. Evolutionary biology 25:279–356.

Valentine, J. W., and C. R. Marshall. 2015. Fossil and transcriptomic perspectives on the origins and success of metazoan multicellularity. Pages 31–46 *in* Evolutionary transitions to multicellular life. Springer, Dordrecht.

Van Valen, L. 1976. Energy and evolution. Evolutionary Theory 1:179–229.

Vogel, S. 1996. Life in moving fluids: the physical biology of flow. Princeton University Press, Princeton, NJ.

———. 2008. Modes and scaling in aquatic locomotion. Integrative and Comparative Biology 48:702–712.

Wan, K. Y., and G. Jékely. 2021. Origins of eukaryotic excitability. Philosophical Transactions of the Royal Society B 376:20190758.

Whelan, N. V., K. M. Kocot, T. P. Moroz, K. Mukherjee, P. Williams, G. Paulay, L. L. Moroz, et al. 2017. Ctenophore relationships and their placement as the sister group to all other animals. Nature Ecology and Evolution 1:1737–1746.

Woollacott, R. M. 1990. Structure and swimming behavior of the larva of *Halichondria melanadocia* (Porifera: Demospongiae). Journal of Morphology 205:135–145.

———. 1993. Structure and swimming behavior of the larva of *Haliclona tubifera* (Porifera: Demospongiae). Journal of Morphology 218:301–321.

Yang, J., M. F. Jansen, F. A. Macdonald, and D. S. Abbot. 2017. Persistence of a freshwater surface ocean after a snowball Earth. Geology 45:615–618.

Ye, Q., J. Tong, S. Xiao, S. Zhu, Z. An, L. Tian, and J. Hu. 2015. The survival of benthic macroscopic phototrophs on a Neoproterozoic snowball Earth. Geology 43:507–510.

Yuan, X., Z. Chen, S. Xiao, B. Wan, C. Guan, W. Wang, C. Zhou, et al. 2013. The Lantian biota: a new window onto the origin and early evolution of multicellular organisms. Chinese Science Bulletin 58:701–707.

Yuan, X., Z. Chen, S. Xiao, C. Zhou, and H. Hua. 2011. An early Ediacaran assemblage of macroscopic and morphologically differentiated eukaryotes. Nature 470:390–393.

Zohary, T., T. Fishbein, M. Shlichter, and L. Naselli-Flores. 2017. Larger cell or colony size in winter, smaller in summer—a pattern shared by many species of Lake Kinneret phytoplankton. Inland Waters 7:200–209.

Zohary, T., G. Flaim, and U. Sommer. 2020. Temperature and the size of freshwater phytoplankton. Hydrobiologia 848:143–155.
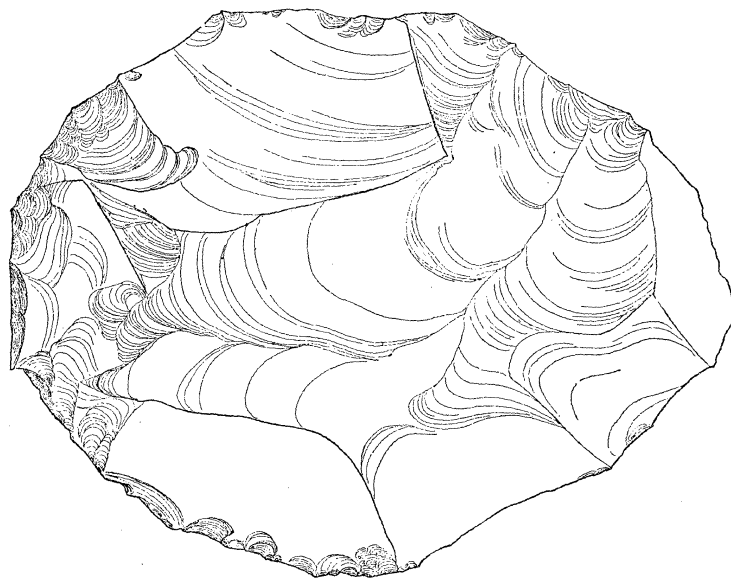
"In ascending Obsidian creek, by way of the newly-cut wagon road which connects Mammoth Hot Springs with the Geyser Basins, we pass first through broad meadows and parked forests. Farther on the valley narrows up and the timber becomes extremely dense. At a point about twelve miles above the junction of the creek with the main stream, there is a narrow gateway known as Obsidian canon, through which the road and creek pass." From "Notes on an Extensive Deposit of Obsidian in the Yellowstone National Park" by Wm. H. Holmes (*The American Naturalist*, 1879, 13:247–250).